We thank Reviewer #1 for their constructive comments. We have listed their comments in bold below and our responses in normal formatting.

Reviewer #1

Firstly, the model only infers the atmospheric CO2 response based on the published relationship between the oceanic inventory change in preformed PO4 and the atmospheric CO2 change. The near-linear relationship between the two is only valid if we assume no solubility and air-sea CO2 disequilibrium effects. I acknowledge that the effects might be implicitly included in the empirical relationship extracted from a few previous global studies. However, I am not sure if the same relationship can be applied to the regional perturbation study. For example, any perturbations in the Southern Ocean (e.g., the ACC band where air-sea CO2 disequilibrium is large due to the short surface residence time of upwelled waters) might not lead to the atmospheric CO2 response proportional to the preformed PO4 response. This point can be especially worrisome because the most sensitive regions turn out to be the ACC band in the study.

Thank you for highlighting this. We have replaced the published preformed PO_4 / CO_2 relationship with one calculated explicitly for this model using an online carbon cycle.

We have tested the impact of CO_2 disequilibrium on the sensitivity results by running an ensemble of experiments where the Martin curve in each region is perturbed individually whilst all others are kept at the control value. The runs have a carbon cycle and so atmospheric CO_2 is predicted as a response to the changing biogeochemistry. The preformed PO_4 and CO_2 from each regional perturbation are plotted over the values from global perturbation experiments (Figure 1). There are minor deviations from the global preformed PO_4 / CO_2 relationship suggesting that disequilibrium effects may be present, but these are relatively minor. The range of CO_2 values predicted by the individual perturbation experiments closely matches the sensitivity patterns from the Latin Hypercube ensemble (Figure 2) further suggesting disequilibrium effects have a minor impact on the results.

We have added these results to the supplementary material that are referenced from a brief discussion of disequilibrium effects in the methods section of the manuscript. We highlight in the discussion that disequilibrium effects may be considered in future analyses.

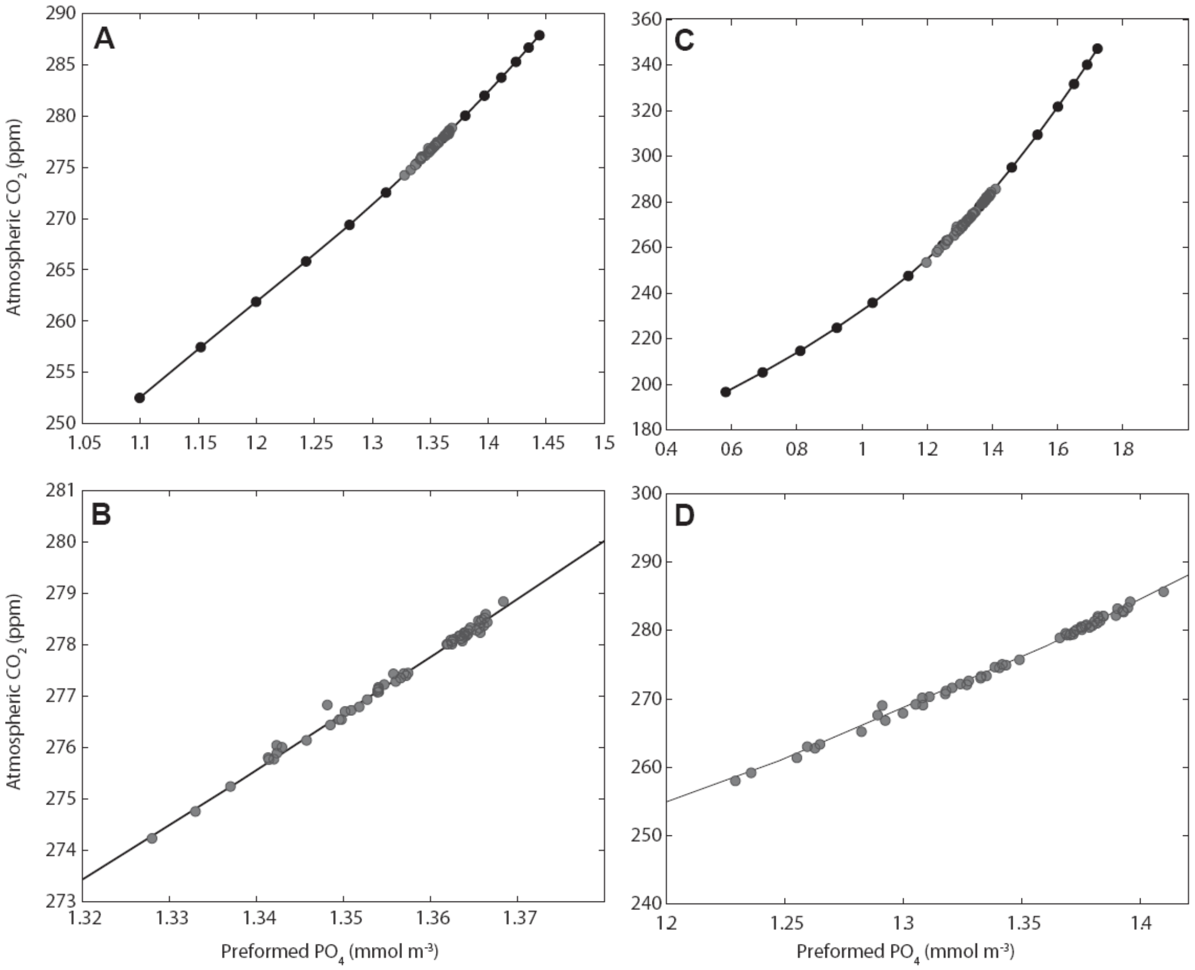

Figure 1. Comparison of CO$_2$ versus preformed [PO$_4$] relationships when the Martin curve is varied as a globally uniform value (black line) from -0.4 to -1.6, and when regions are perturbed individually within the same range (grey). Panels (a) and (b) shows results for the constant-export ensemble with the region of interest expanded in (b). Panels (c) and (d) shows results for the nutrient-restoring ensemble with the region of interest expanded in (d).

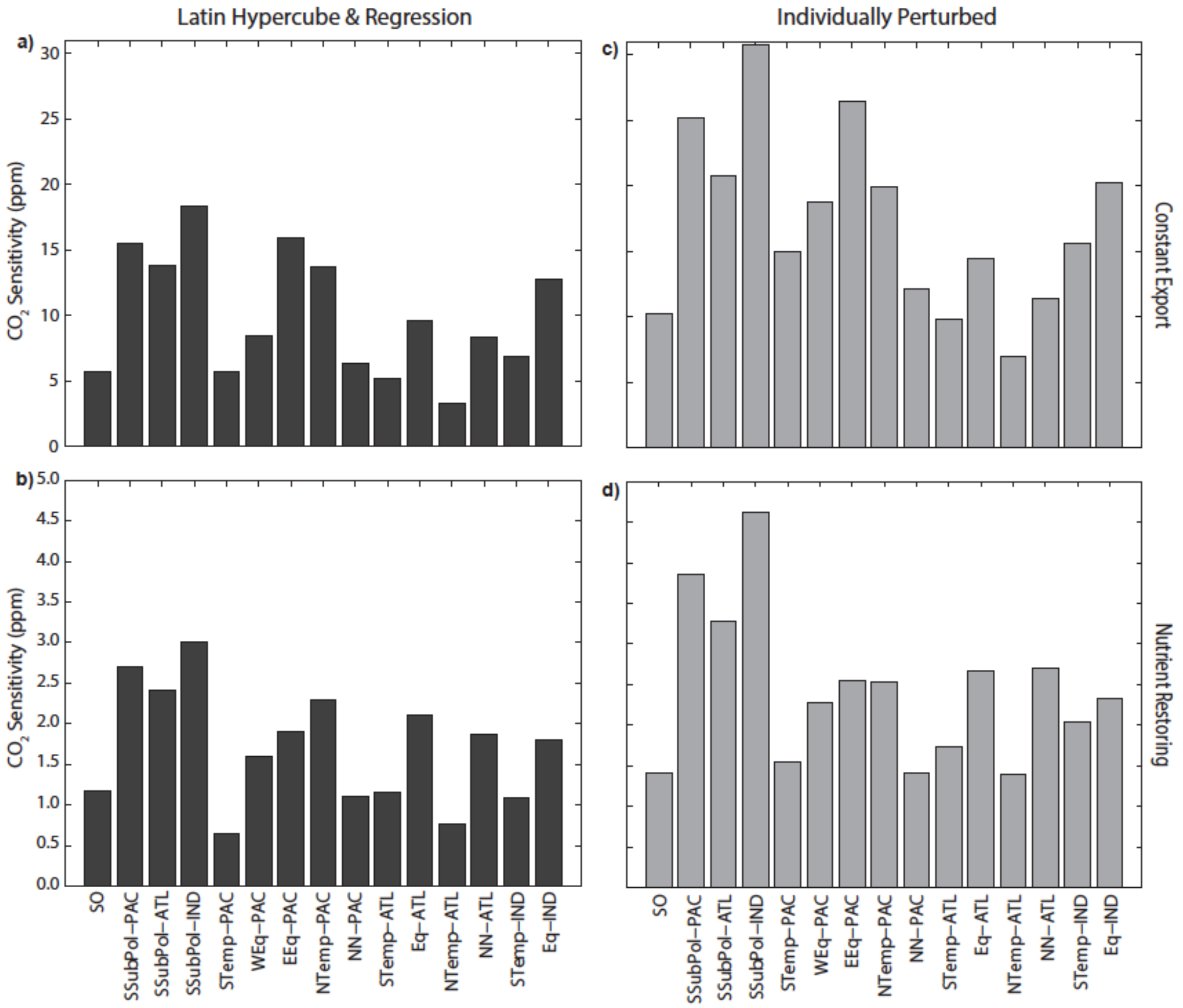

Figure 2. Comparison of CO$_2$ sensitivity estimates from two methods. Black bars are the Latin hypercube and regression-based sensitivity estimates derived with the statistical relationship between preformed PO$_4$ and CO$_2$. Grey bars are the difference between CO$_2$ when each region is perturbed individually from b=0.2 and b=1.6 and atmospheric CO$_2$ is calculated explicitly in the model.

Secondly, the sensitivity is estimated using the multiparameter linear regression method applied to the two sets of 200-member ensemble experiments where 15 regional exponents are perturbed simultaneously. Although the method seems sound, I wonder why the sensitivity should be quantified in this way? Are there any merits? Would the sensitivity be the same or different if the authors perturbed the exponent in a region at a time, requiring a total of 15 perturbation experiments for one model scheme? The individual perturbation experiments seem a simpler and cleaner way to quantify the atmospheric CO2 response to the perturbation and its relations with the export production in each domain.

The reviewer is correct that an alternative approach could be to perturb the remineralisation depth in each region individually (although this would entail at least 4 experiments per region to reasonably characterise the response across the parameter range). The advantage of the Latin hypercube sampling approach is that the resulting sensitivity combines the direct influence of changing remineralisation in one region of interest plus the joint influence of remineralisation changes in other regions, e.g., Pianosi *et al.,* (2016). Given the uncertainty in the observed spatial distribution of remineralisation and the driving mechanisms, we feel it is important to account for the full range of simultaneous changes in remineralisation depths and keep this as the main result.

As per the previous response, we have run the individual perturbation experiments with an explicit carbon cycle. The Martin curve in each region is perturbed to -0.4, -0.7, -1.3 and -1.6 whilst other regions are maintained at the control value of -1.0. Figure 2 shows ΔCO_2 from the -0.4 and -1.6 experiments for each region. The sensitivity patterns match the results from the Latin hypercube ensemble closely. There are differences in magnitude between the two estimates likely due to the fact that there are minor interactions between regions. However, the patterns between regions are preserved. We have added these results in the supplementary as this will provide important context for the key results and strengthen the analysis and interpretation.

Thirdly, the major novel finding is that the highest sensitivity in atmospheric CO2 is to the change in remineralization depth in Subantarctic regions due to high export production and the high connectivity to deep water formation regions. I see the reasoning behind it: The export production should be high because the export will determine how much regenerated PO4 can be affected by the perturbation. The connectivity to deep water formation regions is important because the deep water formation is the main pathway of preformed PO4 to the ocean's interior and the inventory of preformed PO4. However, I am not fully convinced by the authors' finding. Both "nutrient restoring" model and "constant export" model show that the sensitivity of atmospheric CO2 to the remineralization depth change is also high in the "NTemp-PAC" domain (Fig. 3). Yet, the subtropical North Pacific is not a region with high export production nor close to any deep water formation regions. How can it be explained?

Thank you for highlighting this. It is notable that the NTemp-PAC region in general, for this model, does fall along the general trend between export production and sensitivity. In comparison the STemp-PAC region has a much lower sensitivity for a similar export production. This could be related to the age of water masses in the Pacific whereby deeper remineralisation in the STemp-PAC region sequesters organic matter in much younger waters, that will return to the surface ocean faster, thus reducing the sensitivity. We have already noted the range of sensitivity for similar export production in the manuscript, so we have added additional text to discuss this. Overall, because the spatial variability is not overly significant relative to the global uniform variability and because export production is a strong predictor of sensitivity, we have not explored this further.

Similarly, why are the deep water formation regions (i.e., the model NADW and AABW formation regions) not the sensitive regions?

We have added the contribution of preformed PO_4 derived from each region for the control run in Table 1 to help highlight the sensitivity of the deep water formation regions. Kwon et al., (2009) demonstrated that largest changes in preformed PO_4 when changing b globally were associated with deep water formation regions. The updated version of Figure 5 (Figure 4 here), shows that this is in response to changes in b from globally distributed regions (compare colours across the column for SO and NN-Atl regions).

It may be related to the third point. But I don't understand Figure 5. The sensitivity is normalized to what? What do the authors mean by "mean preformed PO4 in a region"? Is it the surface PO4

averaged over each region or the total preformed PO4 subducted from each region divided by the volume of water subducted from the same region?

The "mean preformed PO_4 in a region" is calculated in a similar way to the global preformed PO_4 concentration: the annual mean surface $[PO_4]$ at the end of a simulation is set as a boundary condition and the transport matrix used to calculate the interior distribution of preformed PO_4. In this case, the annual mean surface $[PO_4]$ is set in the region of interest only and the remaining surface has concentrations of zero. The global mean concentration is then calculated from the interior distribution.

Because the absolute magnitude of regional mean preformed PO_4 varies by an order of magnitude across all regions, it is necessary to normalise the concentrations to allow comparison of regression coefficients using the following relationship:

$$\overline{P_{pre}^{region}} = \frac{\overline{P_{pre}^{region}} - \min(\overline{P_{pre}^{region}})}{\max\left(\overline{P_{pre}^{region}}\right) - \min(\overline{P_{pre}^{region}})}$$

In response to this point and to comments from other reviewers, we have revised the format of the figure (see Figure 4 here). We have also updated the text with the description above and the equation to clarify the method of obtaining preformed PO_4 and normalisation.

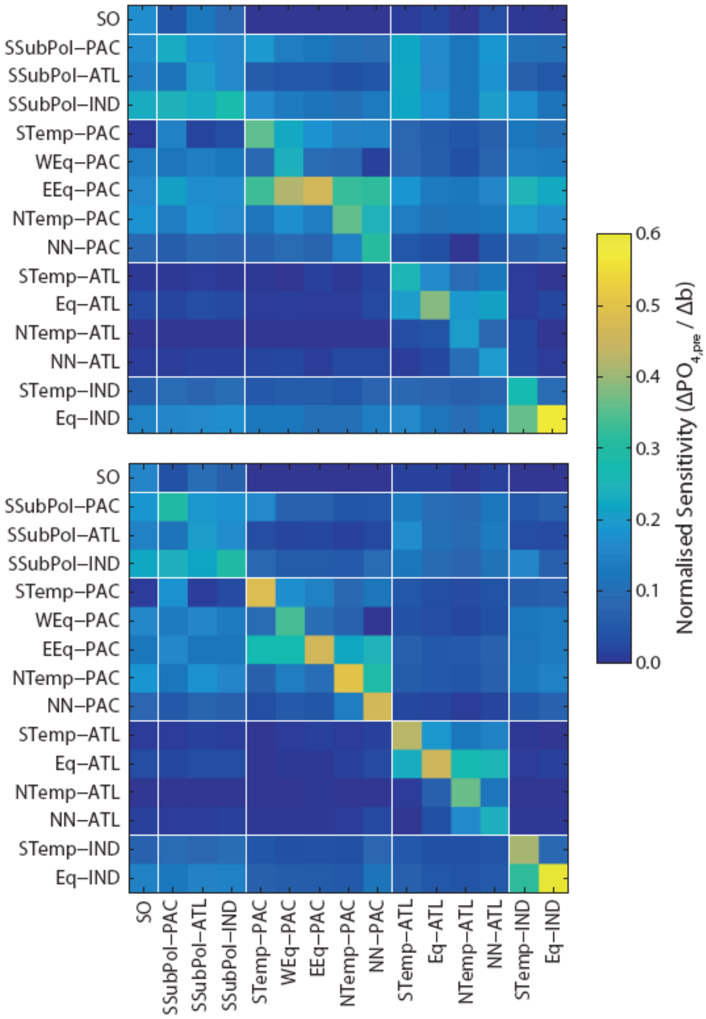

Figure 4. Sensitivity of steady-state normalised mean preformed [PO_4] exported from each region. The preformed [PO_4] from each region is expressed as a function of b using linear regression. Preformed [PO_4] is normalised to the range of values in the ensemble to account for large differences in preformed [PO_4] between regions. The regression coefficients are arranged such that each row shows the impact of changing b in that region on preformed [PO_4] across other regions. Results from the constant-export and nutrient-restoring schemes are shown in the top and bottom panels respectively.

We thank Reviewer #2 for their constructive comments. We have listed their comments in bold below and our responses in normal formatting.

Reviewer #2

My main concern is that the results are likely tied to the circulation model applied. As shown by Duteil et al. (2013; Biogeosciences, 10, 7723–7738, doi:10.5194/bg-10-7723-2013) the transport matrices from the MITgcm seem to suffer from far too large outcrop areas of dense waters in the Southern Ocean (their Fig. 2), indicating that the model circulation does not represent the real ocean in that region very well. Also, because of the very coarse resolution, this model might not represent the physical dynamics in the eastern equatorial Pacific very well. However, in the present study these two regions - the subantarctic regions and equatorial upwelling - have a large influence on CO2 (Fig. 3 and 5). Thus, whereas this study provides important and interesting information for other global model studies that apply similar circulations (as noted in Discussion and Conclusions), I think that a few sentences on this are necessary to caution readers not familiar with the advantages and disadvantages of global circulation models. (To illustrate or investigate this point further, one could, e.g., look at the density distribution or mixed layer depths of the model.)

We have added a plot of density outcrops from the annual mean model output and World Ocean Atlas 13 climatological observations (see Figure 1), a comparison of the volume of water ventilated from each region in the model with the data-constrained estimates from Khatiwala *et al.,* (2012) (Table 1), and a plot of ideal mean age (Figure 2) to the Supplementary Material to demonstrate this caveat.

As the reviewer highlights, the modelled Subantarctic regions are a larger source of water for the ocean interior than observed (Figure 1, Table 1). Additionally, the equatorial regions contribute a much smaller volumetric fraction than observed (Table 1). An alternative approach could be to use the data-constrained ECCO circulation but this comes with a much higher computational cost due to higher resolution and higher number of non-zeros in the sparse matrices, limiting the feasibility of the sensitivity analysis. The MITgcm circulation, as noted by the reviewer, has been widely applied. Therefore, we have kept the MITgcm circulation and have added a substantial discussion in the manuscript referring to the new supplementary figures that discusses the circulation as a caveat to the findings:

"Our results are dependent on the use of transport matrices derived from one global circulation model. Whilst this model has been widely applied to study biogeochemistry previously, it is subject to a number of caveats. The ocean model predicts significantly larger outcrops of dense water in the Southern Ocean compared to observations (see Figure S4; Duteil et al., 2013) leading to deep-water formation occurring at latitudes around 50S (Figure S5). The volumetric fraction of water in the ocean interior derived from the Subantarctic is also higher (26%) compared with data-constrained estimates (18%: Khatiwala et al., 2012). As such, the sensitivity estimates for the Subantarctic may be over-estimated. This is also consistent with the higher sensitivity compared to the basin-scale analysis of Kwon et al., (2009) who found that the Southern Ocean (>40S contributed 22% of the global CO_2 sensitivity, compared with 36% in this study (>38S, Table 1). However, our results have key similarities, including absolute and relative magnitudes of regional preformed PO_4 export, to other studies using alternative steady-state circulation states (DeVries et al, 2012; Pasquier and Holzer 2016). As such, our results should be broadly reproducible with other models."

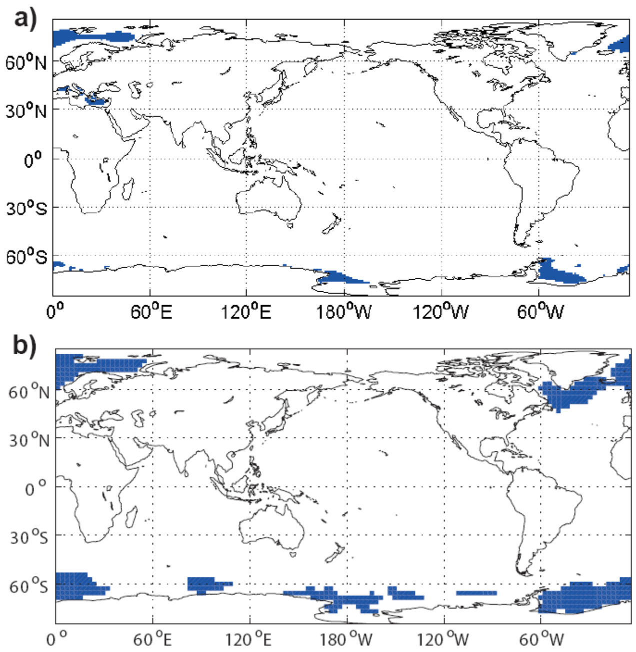

Figure 1: Regions where density is greater than 1027.5 kg m^{-3} calculated using the Gibbs SeaWater toolbox (McDougall & Barker 2011) with annual-mean temperature and salinity from (a) World Ocean Atlas 18 and (b) MITgcm output.

Figure 2. Meridional cross section of ideal age in the Pacific (224°W).

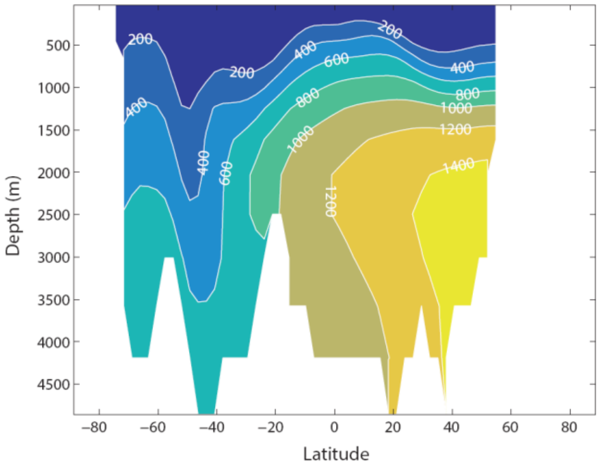

Table 1. Global ocean volumetric fraction (%) for different source regions from a data-constrained estimate (Khatiwala *et al.,* 2012) and from this study.

Region	**Khatiwala2012 (%)**	**This Study (%)**
Antarctic	39	28.7
Subantarctic	18	26.1
North Atlantic	26	35
Tropical	4.5	0.86
Subtropics	8.1	4.5
NPacific	4	4.5

There seems to be a strong sensitivity of CO2 to changes in b in the constant-export scheme (Fig 3), and also a clear relationship to export (Fig 4a). In contrast, normalized (by what?) preformed phosphate seems to be more sensitive in the nutrient restoring scenario (Fig 5 vs Fig S3), and no relationship seems to exist between CO2 sensitivity and export (Fig 4b). I think these contrasting patterns for both model types deserve a bit more discussion. Perhaps some section plots of, e.g., density across the Pacific and Atlantic (see above) could aid the disussion about the effects of circulation vs. export type ("biogeochemistry"). If the circulation model is anywhere near the real world, some insight regarding the "connectivity" of different regions might perhaps be gained from the data-constrained analysis of water fractions presented by Khatiwala et al. (2012; Earth and Planetary Science Letters, 325–326, 116–125)

In response to this and other reviewer comments, we have replotted Figure 5 in a format which is hopefully more accessible, and that allows for the inclusion of panels for both the fixed and restoring export ensembles (see Figure 3 here). The new plot highlights that the sensitivity estimates are broadly similar across both the nutrient-restoring and constant-export schemes but that preformed PO_4 appears more sensitive to local changes in b (boxes on the diagonal) in the nutrient-restoring scheme. We have added text in the Results to note this difference. We have also included the following equation in the manuscript text to describe the normalisation:

$$\overline{P_{pre}^{region}} = \frac{\overline{P_{pre}^{region}} - \min(\overline{P_{pre}^{region}})}{\max\left(\overline{P_{pre}^{region}}\right) - \min(\overline{P_{pre}^{region}})}$$

We have addressed the comments on circulation in the response to the previous comment.

In terms of the relationship between sensitivity and export production, the distribution of regions within the nutrient-restoring panel is very similar to the constant-export panel despite a much weaker relationship. We have added text to the Results to demonstrate the weaker relationship between export production and sensitivity for the nutrient-restoring scheme:

“Similarly, we find a general positive correlation between sensitivity and regional export production ($r=0.79$, $p<0.01$ for constant export, $r=0.47$, $p=0.07$ for restoring uptake), as measured by the mean annual average export production across the 200 ensemble runs (Fig 4). The correlation is much weaker with nutrient restoring uptake compared to the constant-export production.”

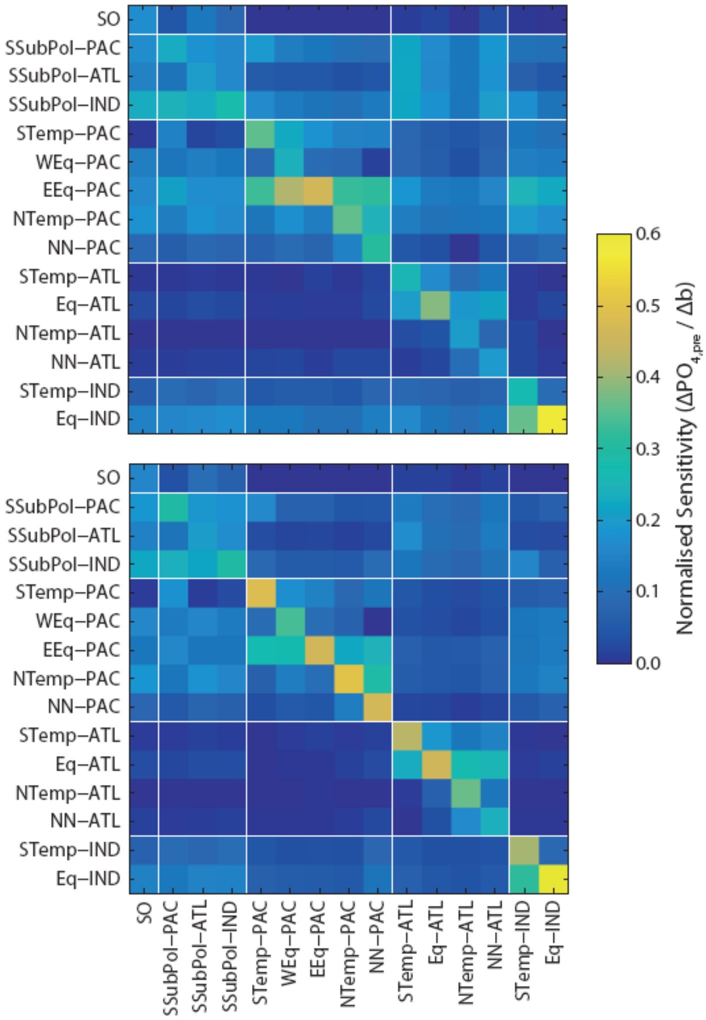

Figure 3. Sensitivity of steady-state normalised mean preformed [PO_4] exported from each region. The preformed [PO_4] from each region is expressed as a function of b using linear regression. Preformed [PO_4] is normalised to the range of values from each region within the ensemble to account for large differences in preformed [PO_4] between regions. The regression coefficients are arranged such that each row shows the impact of changing b in that region on preformed [PO_4] across other regions. Results from the constant-export and nutrient-restoring schemes are shown in the top and bottom panels respectively.

p 3, line 15: "MITgcm" sounds like technical slang to me - is there a better word for it?

The text has been changed to: *“MIT general ocean circulation model (MITgcm)”*

Section 2.3: At first, I had difficulties understanding the experimental design; I would suggest to indicate more clearly that the "reference" experiments were carried out over a discrete set of

globally uniform "b" values (how many?), and to distinguish this more clearly from the LHS experiments for the regional variation

We have updated the text with headings to separate the description of the control run, global and regional sensitivity runs. We have also clarified the number of globally uniform b values tested.

Eqn. 2 and Table 1: The connection between beta_0 and beta_k of Eqn 2 and Table 1 is not clear to me: are beta in the table beta_k of equation 2? Is beta_0 constant?

We have added the subscripts to the betas in Table 1 and have added a reference to eqn. 2 in the Table caption.

p 5, line 11: "we fit linear regression models" - I suggest to refer here again to Eqn 2.

Done.

p 5, line 28-29: "However, the relative sensitivity ranked across regions remains similar, as shown by expressing b_k as a percentage (Table 1)." - relative to what?

This has been reworded to "…as shown by expressing each β_k as a percentage of $\sum_k \beta_k$ (Table 1)."

Table 1: Please explain clearly what is shown in this Table: are beta the beta_k of Eqn 2? What does beta(%) mean - normalised by area? Are the two rightmost columns for the constant export experiments?

We have added the subscripts to the betas in Table 1 and have added a reference to eqn. 2 in the Table caption. We have also added annotation and text to the caption to explicitly state that the beta(%) is relative to the sum of the regression coefficients.

p 6 line 4 "positive"

Fixed.

p 6 second paragraph: is there a difference between "export production" and "export productivity"?

Fixed. Export production is now used throughout.

p 6, line 20 "is normalised" - by what?

The text has been updated to explicitly describe the normalising (see also equation above)

p 7 line 3: "sensitivity"

Fixed.

p 11, line 5: "κ"

Fixed.

p 11, line 20: "function"

Fixed.

p 19, caption: "relects"?

Fixed to "reflects".

We thank Reviewer #3 for their constructive comments. We have listed their comments in bold below and our responses in normal formatting.

Reviewer #3

While I understand why the two model scenarios (restoring or fixed export) are presented as end-members, the fixed export run nevertheless takes its export from a restoring run. It is true that output from the run giving the closest fit to observations is used as baseline but it should still be acknowledged that the 'end-members' are far from independent models.

We have amended the text as follows: "These two schemes represent two end-member scenarios, strictly within the context of this model, where organic matter production either depends entirely on macronutrient concentrations…"

The description of tracking preformed phosphate needs more detail. The decomposition described in Appendix B gets phosphate away from surface only – it still needs to be tracked in the interior. How is this done?

We have changed equation B1 in Appendix B to make the operation clearer:

$$\boldsymbol{PO_4^{pre}} = (\boldsymbol{A_i^I A_e^I} - \boldsymbol{I})^{-1}((\boldsymbol{A_i^I B_e} + \boldsymbol{B_i})\boldsymbol{PO_4})$$

The authors should show the scatter plot of predicted vs observed values for the relationship described in page 5 lines 12-13 as it is fundamental to the manuscript. It should show predicted and observed changes in PO4 as this is the predicted field.

We have added this figure to the manuscript, (see Figure 1 here).

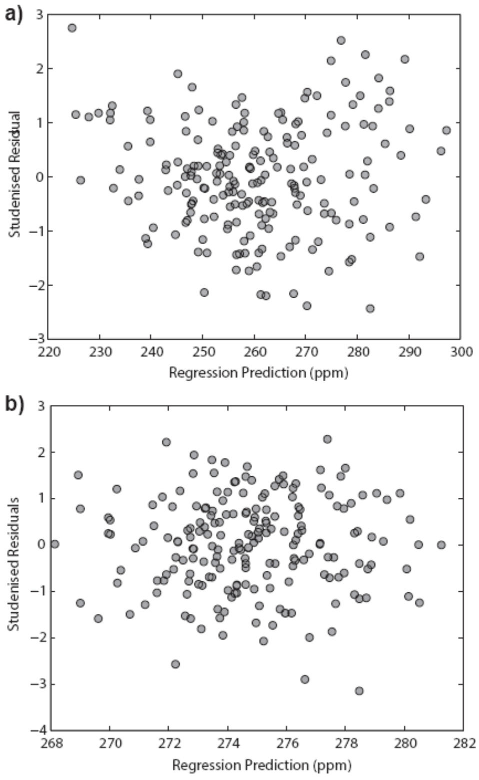

Figure 1. Residuals for the linear regressions that estimate sensitivity of CO_2 to spatially varying Martin curves for (a) constant-export and (b) restoring-uptake schemes.

Fig 6 and section 3.2 – there is a sound argument for geometric mean so just show geometric mean and give the argument in the methods. It is not necessary to show arithmetic mean results in Fig 6a

We have moved this figure panel to the discussion of calculating the geometric mean in the supplementary material.

As a more informative second panel for Fig 6 show the same as current 6b but with regression taken out to show variability due to regional variability more clearly. The authors should also acknowledge in the text that the random sampling leads to undersampling of highest and lowest global b values.

Thank you for this suggestion. Because the global mean of responses track the globally-uniform responses closely and we could not find any evidence that the variability was associated with changes in b in any specific region, this additional plot did not provide much additional information so we have kept the original panel.

We have added the following text: "Note that b in each region is varied within the full parameter range but that because Latin hypercube sampling varies all parameters across their parameter range simultaneously the global mean does not reach the highest and lowest global b values."

How independent in structure are the 3 models used for the PO4 vs pCO2 relation?

In response to other reviewer comments we have replaced the statistical relationship between preformed PO_4 and CO_2 with one calculated specifically for this model using a carbon cycle.

Fig A1 should be in the main body of the paper

We have moved the equivalent plot to the Methods section of the manuscript.

Consistency needed in terminology: in Subantarctic (text) and subpolar (fig)

We have changed any use of 'subpolar' to 'Subantarctic' throughout.

Remineralisation depth is defined (page 2, lines 8-9) assuming exponential profile (decrease by 63%) but models use Martin curve

The reviewer is correct that the definition assumes exponential decay whereas the Martin curve is a power-law. This was used previously by Kwon *et al.,* (2009) who used Martin curves but also expressed them as e-folding depths. Our purpose was to introduce the term 'remineralisation depth' as this allows for more clear and concise discussion of changes in Martin curves as the terms 'shallower' or 'deeper' can be used rather than changes in the dimensionless exponent b.

We have changed the text to better reflect this comment:

"In this paper we use the term 'remineralisation depth', defined as a depth at which a defined % of POC has been remineralised. Previously, this has been defined as an *e*-folding depth: the depth at which ~63% of POC has been remineralised (Kwon et al., 2009) (although note the Martin curve is not exponential)."

Does the misfit function used to carry out the comparison to WOA (page 4, lines 22-23) take volume into account?

Yes. We have amended the text to state that it is volume-weighted.

Explain the maximin Matlab option for hypercube sampling in Matlab (page 4, line 31)

We have added the following text to clarify:

"…with 'maximin' sampling (an additional constraint that helps reduce clustering of samples, by maximising the minimum distance between points, in order to give a well-spread distribution of points across the parameter space)."

page 4 line 25: not sure that "reference" is appropriate

We have updated the experiment description with headings to separate the description of the control run, global and regional sensitivity runs. "Reference" has been removed from the text.

Fig 3 caption needs rewording. All values are positive.

The caption has been reworded to: "The sensitivity value reflects the increase in CO_2 (preformed PO_4) for an increase in b (shallower remineralisation)."

The authors' definition of the Subantarctic boundary makes it a little difficult to compare results to Kwon's paper where the Southern Ocean was defined as south of 40S. Given that the Kwon paper provides such strong motivation for this manuscript this deserves comment.

We had added an additional row to Table 1 in the manuscript describing metrics for the Southern Ocean as defined as >38°S for comparison with Kwon et al., (2009). We have also noted this comparison in the Discussion.

Page 6, lines 4-6: It should be explicitly acknowledged that there is a rather weak relationship between export and sensitivity for the restoring runs (Fig 4b)

We have added correlation coefficients to help demonstrate the weaker relationship between export and sensitivity. The following text has been added:

"Similarly, we find a general positive correlation between sensitivity and regional export production ($r=0.79$, $p<0.01$ for constant export, $r=0.47$, $p=0.07$ for restoring uptake), as measured by the mean annual average export production across the 200 ensemble runs (Fig 4). The correlation is much weaker with nutrient restoring uptake compared to the constant-export production."

Use notation that distinguishes regional and global means of PO4_pre

We have updated the text with notation to distinguish between regional and global means of preformed PO_4.

Both constant export and nutrient restoring should be shown in Fig 5.

In response to other comments from reviewers, we have updated the format of this figure and have added panels for both constant export and nutrient restoring.

Page 7, Line 3: "sensitivity"

Fixed.

Page 8, lines 28-30: "As such, the global mean change in potential future and past changes in remineralisation depth may be larger than the uncertainty associated with spatial variability." B changes discussed less than current observed range" The changes being discussed here are substantially smaller than the current range of observed values. Even if, as this paper argues, the global ocean may not be overly sensitive to spatial variation in b, it is worth noting that the current uncertainty in a global value of b still has very large uncertainty partly because of the confounding effect of under-sampled spatial variability

We have added the following text: “However, we note that the modern global mean b is subject to uncertainty associated with under-sampled spatial variability.”

Page 10, line 21: Which sea ice field is used?

The following text has been added:

“…scaled the fraction of seaice present (Fice, as monthly average fields from the original circulation model).”

Page 11, line 5: 1-v not 1-kappa

Fixed.

Appendix A: state that the bottom of the second grid box in the vertical is at 120m (presumably)?

Done.

We thank Reviewer #4 for their constructive comments. We have listed their comments in bold below and our responses in normal formatting.

Reviewer #4

First, I am concerned that biases in the circulation model might skew the results and have not been properly acknowledged. Can the authors state whether they are using a new version of the MITgcm 2.8degree circulation model, or the same one that has been used since the early OCMIP era? Previous studies (Dutay et al. 2002; Doney et al. 2004) have identified some significant shortcomings of this circulation model that might impact the relative importance of different regions in the current study. Not least, the model does not produce deep water along the Antarctic coastline as it should, and instead produces deep water at around 50S. This would shift deep water formation from the Antarctic to the Subantarctic regions defined in the current study, and give the Subantarctic region unrealistic leverage over interior nutrient distributions. It could be the case that the circulation has been reformulated since those studies and this bias corrected. If that's the case it is important for the authors to demonstrate this, to reassure readers like myself who have reservations about that model. The simplest way to show this would be to calculate ideal age in their model, and plot a meridional cross section through the Pacific. They should be able to show a tongue of young water subducting right along the Antarctic coastline and spreading northwards along the seafloor (not a tongue of young water penetrating the deep ocean at 50S). If they are indeed using the old, biased circulation model, this should be acknowledged in the text where the significance of the Subantarctic region is discussed. Either way, a figure like the one I suggested should be included as a supplementary figure either to demonstrate that the circulation model is robust, or to make readers aware of potential biases introduced by the Southern Ocean wartermass structure.

Thank you for highlighting this important caveat. We have plotted the meridional cross section (Figure 1) and the model does subduct water around 50°S. In response to this, and to comments from other reviewers, we have included this figure, a comparison of where the densest surface waters are versus observations, and a water-mass analysis in the supplementary material. We have also updated the Discussion in the manuscript to make clear that this is an important caveat. We have kept the circulation model for a number of reasons: 1) the Subantarctic regions do not dominate the sensitivity at a global level, 2) the circulation model is likely to over-estimate the sensitivity of CO_2 to remineralisation in the Subantarctic regions, 3) it is widely used for modelling biogeochemistry.

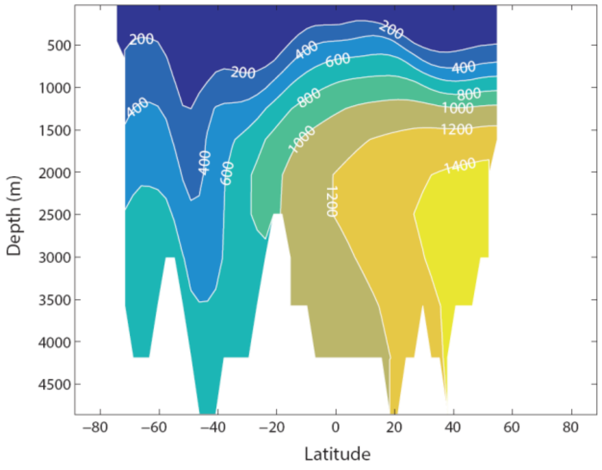

Figure 1. Meridional cross section of ideal age in the Pacific (224°W).

Second, I am confused as to why a paper focused on sensitivity of atmospheric CO2 does not use a model that resolves the carbon cycle. Instead, they model only the phosphorous cycle and relate it to carbon cycle changes using a relationship derived from prior modeling studies. The authors state that this is to avoid the computational expense of simulating the carbon cycle. But that would only require the addition of two tracers – DIC and Alk, and a single value for a well-mixed atmospheric CO2 concentration. This should therefore only double the computation time, and given that transport matrix method is being used (where efficient Crank-Nicolson time-stepping methods can be applied), this does not seem preclusive. And even then, they needn't include the carbon cycle in all 200 of their simulations, only enough to redefine the statistical PO4 vs. CO2 relationship from their own model. This would at least keep their study self-consistent, rather than relying on previous results from different models. If the authors are not able to do this in the current study (which would be preferable), they should again acknowledge more clearly the caveats of their chosen method. In Fig. A1, it is obvious that different models yield different relationships between these properties. Fitting just the Marinov et al. results would lead to a much shallower relationship, but those results are not strongly weighted because they contribute fewer data points than others. It would seem more reasonable to fit the relationship for each previous study separately, and propagate that uncertainty into their CO2 estimates

In response to this comment, and to comments from other reviewers, we have added the carbon cycle to the model. We have redefined the preformed PO_4 and CO_2 relationship and have used this to calculate the change in CO_2 for the Latin hypercube ensemble.

Figure 3. I think a bar plot would be better suited to show this data. This is a key result of the paper, and a quantitative comparison between regions and production methods would be simpler in a bar format.

Thank you for this suggestion. We have added additional panels to the figure showing the sensitivity estimates in a bar format (Figure 2).

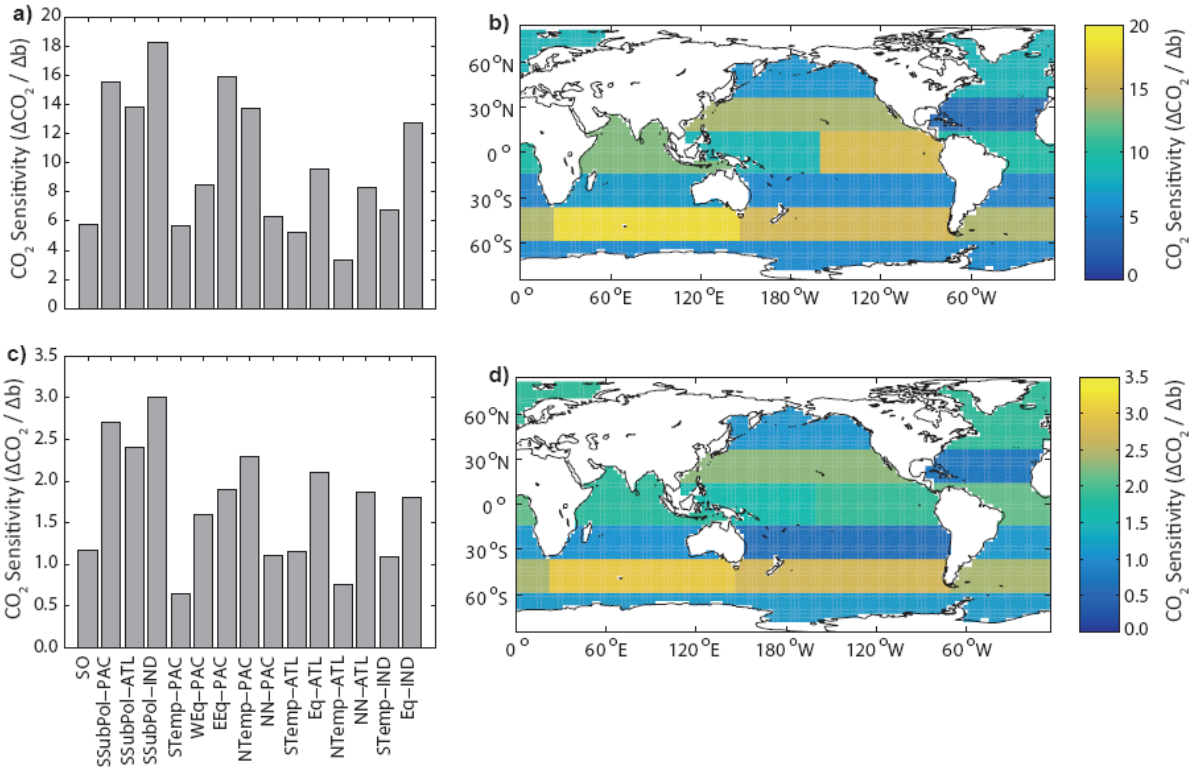

Figure 2. Regional sensitivity (ΔCO_2 / Δb) of atmospheric CO_2 (ppm) to changes in Martin curves for the constant-export scheme (panels a & b) and restoring-uptake scheme (panels c & d). Atmospheric CO_2 is inferred from modelled preformed PO_4 using empirical relationships.

Figure 5. This figure is a little overcomplicated, as evidenced by the fact that a fair amount of the text (not just the caption) is devoted to explaining what it means. How about showing these results as a color matrix instead? Region in which b is varied down the rows, region in which we are looking at the preformed PO4 along the columns (or vice versa), color shows the regression coefficient. I know this is contrary to my previous comment about bars being more precise, but I think precision is less important here than the need to reduce complexity. The color matrix would allow the reader to pick out "bright" rows or columns as indicative of important regions.

Thank you for this useful suggestion. We have reformatted the figure as a matrix (Figure 3). This does highlight spatial patterns more clearly and allows both constant-export and nutrient-restoring results to be shown.

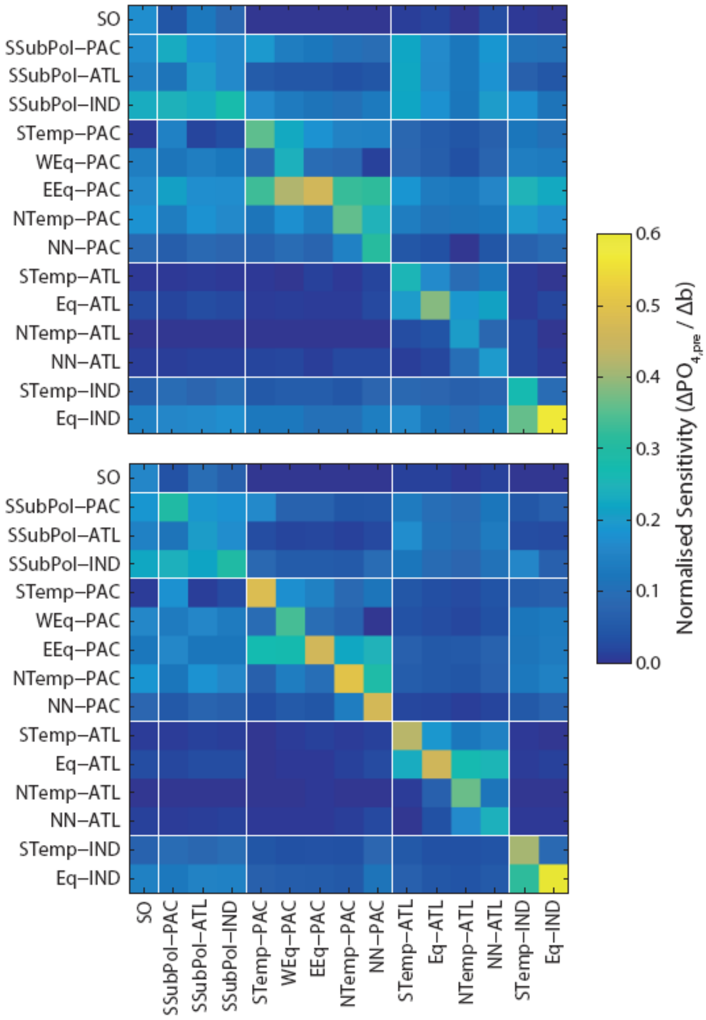

Figure 4. Sensitivity of steady-state normalised mean preformed [PO_4] exported from each region. The preformed [PO_4] from each region is expressed as a function of b using linear regression. Preformed [PO_4] is normalised to the range of values in the ensemble to account for large differences in preformed [PO_4] between regions. The regression coefficients are arranged such that each row shows the impact of changing b in that region on preformed [PO_4] across other regions. Results from the constant-export and nutrient-restoring schemes are shown in the top and bottom panels respectively.

Section 3.2 and Figure 6. I'm not sure why the results in Figure 6a are shown? The authors acknowledge that simply averaging the b values is not the correct way to quantify the global-mean remineralization profile, and then attempt to correct for it in panel b. But why show an obviously incorrect result in the first place? It seems like the correct way to define a "global mean b-value" would be to construct a global-mean (area-weighted) organic matter flux profile, and then fit the Martin relationship to that.

We have moved panel a to the discussion of averaging in the supplementary material. We have kept the averaging approach as this has been used previously, e.g., Henson et al., (2012), and so provides useful context.

Sensitivity of atmospheric CO_2 to regional variability in particulate organic matter remineralization depths

Jamie D. Wilson[1,2], Stephen Barker[2], Neil R. Edwards[3], Philip B. Holden[3], and Andy Ridgwell[1,4]

[1]BRIDGE, School of Geographical Sciences, University of Bristol, UK
[2]School of Earth and Ocean Sciences, Cardiff University, UK
[3]School of Environment, Earth and Ecosystems, Open University, UK
[4]Department of Earth Sciences, University of California, Riverside, USA

Correspondence: Jamie D. Wilson (jamie.wilson@bristol.ac.uk)

Abstract.

The concentration of CO_2 in the atmosphere is sensitive to changes in the depth at which sinking particulate organic matter is remineralised: often described as a change in the exponent "*b*" of the Martin curve. Sediment trap observations from deep and intermediate depths suggest there is a spatially heterogeneous pattern of b, particularly varying with latitude, but disagree over the exact spatial patterns. Here we use a biogeochemical model of the phosphorus cycle coupled with a steady-state representation of ocean circulation to explore the sensitivity of preformed phosphate and atmospheric CO_2 to spatial variability in remineralisation depths. A Latin hypercube sampling method is used to simultaneously vary the Martin curve indepedently within 15 different regions, as a basis for a regression-based analysis used to derive a quantitative measure of sensitivity. Approximately 30% of the sensitivity of atmospheric CO_2 to changes in remineralisation depths is driven by changes in the Subantarctic region (36°S to 60°S), simliar in magnitude to the Pacific basin despite the much smaller area and lower ~~productivity~~export production. Overall, the absolute magnitude of sensitivity is controlled by export production but the relative spatial patterns in sensitivity are predominantly constrained by ocean circulation pathways. The high sensitivity in the Subantarctic regions is driven by a combination of high export production and the high connectivity of these regions to regions important for the export of preformed nutrients such as the Southern Ocean and North Atlantic. Overall, regionally varying remineralisation depths contribute to variability in CO_2 of between $\pm$ 5 - 15 ppm relative to a global mean change in remineralisation depth. Future changes in the environmental and ecological drivers of remineralisation, such as temperature and ocean acidification, are expected to be most significant in the high latitudes where CO_2 sensitivity to remineralisation is also highest. The importance of ocean circulation pathways to the high sensitivity in Subantarctic regions also has significance for past climates given the importance of circulation changes in the Southern Ocean.

1 Introduction

Sinking particles of organic matter transfer 5-10 Pg C per year from the upper ocean to the ocean interior (Henson et al., 2011), as part of a process known as the biological pump. As these particles sink, they are remineralised through bacterial and zooplankton-related activity, releasing the carbon and nutrients back into solution at depth. Vertical fluxes of particulate organic carbon (POC) in the water column have historically been described by the Martin Curve, a power-law function that describes the rapid decrease in flux (F_z) from a maximum value at depth z_0, nominally the base of the mixed layer, to a small asymptotic value in deep waters (equation 1: Martin et al., 1987) (Fig. 1):

$$F_z = F_{z_0}\left(\frac{z}{z_0}\right)^{-b} \tag{1}$$

The dimensionless exponent in the power-law (‘b’) describes whether organic matter is remineralised predominantly at shallower depths (larger values of b, e.g., b=1.6) or deeper ~~depths~~ in the water column (smaller values of b, e.g., b=0.4) (Fig. 1). The exponent itself parameterises the rate at which POC sinks through the water column (units of m day^{-1}) and the rate at which it is remineralised (units of day^{-1}) (Kriest and Oschlies, 2008; Lam et al., 2011). In this paper we use the term ‘remineralisation depth’, defined as a depth at which a defined % of POC has been remineralised. Previously, this has been defined as an e-folding depth: the depth at which ∼63% of POC has been remineralised (Kwon et al., 2009) ~~, to refer to changes in POC remineralisation as it is relatable to alternative mathematical functions also used (e.g., Cael and Bisson, 2018)~~(although note the Martin curve is not exponential).

Ocean biogeochemical models predict that the concentration of CO_2 in the atmosphere is sensitive to changes in a globally uniform remineralisation depth. Kwon et al. (2009) showed that a deepening of the remineralisation depth globally of 24 m (from b =1.0 to 0.9), redistributed dissolved inorganic carbon (DIC) from the intermediate waters to the deep ocean leading to a reduction in atmospheric CO_2 of between 10 and 27 ppm. The drawdown was also associated with a decrease in the global mean concentration of preformed nutrients in the ocean interior (nutrients that are not utilised by biology in the surface ocean and enter the ocean interior via circulation: Ito and Follows, 2005). Kwon et al. (2009) found that an increase in respired carbon in the deep ocean was balanced by a reduction in preformed nutrients exported in the North Atlantic. Deepening of the POC remineralisation depth could also drive dissolution of calcium carbonate ($CaCO_3$) in ocean sediments ultimately drawing down more CO_2 over millennial timescales (Roth et al., 2014). The potential impact of remineralisation depth changes on atmospheric CO_2 is therefore a highly relevant component of the marine carbon cycle for both past and current changes in climate (Riebesell et al., 2009; Hülse et al., 2017; Meyer et al., 2016).

Analyses of global sediment trap observations suggest there is a spatially heterogeneous pattern of remineralisation depths in the modern ocean that varies particularly with latitude. A synthesis of observations from deep sediment traps (>1500–2000 m: Henson et al., 2012) suggests that POC fluxes in high latitudes attenuate faster with depth (shallower remineralisation depth: b=1.6) than in low latitudes, where a greater proportion of POC is transported to depth (deeper remineralisation depth: b=0.4), (Fig. 1). However, POC fluxes measured using neutrally buoyant sediment traps at shallower depths (<1000 m) suggest the inverse of this latitudinal pattern (Marsay et al., 2015) (see also, Weber et al., 2016). A recent compilation of sediment trap data and profiles of particle size distributions observed in the water column highlight additional intra-basin variability in b (e.g., shallower remineralisation in the East Equatorial Pacific than in the West) and inter-basin variability (e.g., deeper remineralisation in the Atlantic and Indian basins compared to the Pacific) (Guidi et al., 2015). The uncertainty in the spatial variability of remineralisation depths presents a challenge for determining which mechanisms may be responsible for changes in remineralisation depths and how these might drive future or past changes in remineralisation (e.g., Boyd, 2015). Additionally, this also presents a challenge for biogeochemical models that are beginning to resolve the mechanisms that are potentially responsible for these spatial patterns such as particle size dependent sinking rates (DeVries et al., 2014), temperature dependent remineralisation (John et al., 2014), and oxygen dependence (Laufkötter et al., 2017).

A key question in light of the observed spatial variability in remineralisation depths and the associated uncertainty in spatial patterns is: what is the sensitivity of atmospheric CO_2 concentrations to spatial variability in remineralisation depths? Kwon et al. (2009) further quantified the sensitivity of atmospheric CO_2 to basin scale changes in remineralisation depths by perturbing them in each basin individually, finding that the Pacific, Southern Ocean (defined as >40°S), Atlantic and Indian Oceans contributed 38%, 22%, 21% and 19% of the total CO_2 drawdown respectively (Kwon et al., 2009). The variability in CO_2 sensitivity between basins matched the variability in the magnitude of export production integrated over the basins and basin area, suggesting that no one region was more significant when varying the globally uniform remineralisation depth (Kwon et al., 2009). However, this basin-scale analysis does not resolve the sensitivity of atmospheric CO_2 occuring at the resolution suggested by observations, i.e., a latitudinal and within-basin scale, or at the resolution of ecological and biogeochemical variability (Longhurst, 1998; Fay and McKinley, 2014). Additionally the analysis does not allow for the identification of potential interactions and feedbacks between regions when remineralisation depths are changing simultaneously.

Here we aim to address these issues by performing a global sensitivity analysis of regionally varying remineralisation depths. To this end, we use ~~the 2.8° resolution MITgcm~~ a transport matrix (a steady-state computationally efficient representation of ocean transport) derived from the MIT global circulation model (MITgcm) with a model of phosphorus and carbon cycling where the ocean is divided into 15 regions in which remineralisation depths can change independently. Remineralisation depths are perturbed simultaneously using Latin hypercube sampling and sensitivity quantified using regression analysis,~~and related to changes in atmospheric CO_2 via preformed nutrients~~.

2 Methods

2.1 Model Description

We provide a brief description of the model here and a more detailed description in Appendix A. The approach to quantifying sensitivity used here relies on the ability to run an ensemble of model experiments. To make this approach feasible we use the ‘transport matrix method’ (Khatiwala et al., 2005; Khatiwala, 2007), a steady-state computationally efficient representation of ocean transport and climate derived from a ~~dynamic ocean~~ global circulation model. We use monthly mean transport matrices derived from the 2.8° global configuration of the MIT ~~ocean model~~ global circulation model (MITgcm) with 15 vertical levels (Khatiwala et al., 2005; Khatiwala, 2007). These specific matrices have been previously applied to model biogeochemistry (Kriest et al., 2012; Kriest and Oschlies, 2015).

The biogeochemical model used here is a model of the marine phosphorus and carbon cycle that resolves phosphate (PO_4~~)and~~), dissolved organic phosphorus (DOP), ~~similar to other models used to quantify the sensitivity of the biological pump (DeVries et al., 2012, 2014; Pasquier and Holzer, 2016)~~dissolved inorganic carbon (DIC), total alkalinity and atmospheric CO_2.

Following Kwon et al. (2009), we calculate the production of organic matter using either a nutrient-restoring scheme, where $[PO_4]$ is restored to monthly observations of $[PO_4]$ (Garcia et al., 2014) with a timescale of 30 days (eqn. A3), ~~and one~~ or with constant export production where export production is fixed to that of ~~the control run unless~~ a previous run unless local nutrients fall below zero. These two schemes represent two end-member scenarios, strictly within the context of this model, where organic matter production either depends entirely on macronutrient concentrations and can increase with higher nutrient fluxes (restoring) or is limited by other factors such as light or micronutrients (constant export). The remineralisation of particulate organic ~~phosphorus (POP)~~ matter is parameterised using the Martin curve (eqn 1). ~~We use~~ To further facilitate a large number of experiments for the sensitivity analysis, we use the model to define a statistical relationship between preformed PO_4 (~~PO_4^{pre}) to relate changes in the modelled phosphorus cycle to changes in~~ P_{pre}) and atmospheric CO_2 ~~using a statistical relationship derived from published experiments (Appendix~~ and run the model with a phosphorus cycle only (see Section A0.2). ~~This provides a way of relating changes in our model of phosphorous to changes in atmospheric CO_2 without simulating a relatively computationally expensive carbon cycle.~~

2.2 Experiment Design

2.2.1 Defining Regions

We define a set of oceanic regions to approximately encapsulate the large-scale variability in biogeochemistry and patterns of remineralisation depths observed in sediment trap studies. We define regions by lines of latitude and basins, similar to the approach used by air-sea flux inversion studies, e.g., (Gloor et al., 2001; Mikaloff Fletcher et al., 2006). 15 regions are defined based on a partitioning by Gloor et al. (2001) with some minor changes (Fig. 2a). The assigned regions broadly correspond with major features in observed surface $[PO_4]$ such as higher concentrations in upwelling regions and lower concentrations in the nutrient-depleted gyres (Fig. 2b). This suggests the regions should be a reasonable analogue for an alternative ~~approaches that capture~~ approach that captures key spatial variability in ecology and biogeochemistry by defining regions using vertical mixing, mixed layer depths, sea ice and sea surface temperature (Longhurst, 1998; Sarmiento et al., 2004; Henson et al., 2010; Fay and McKinley, 2014). The regions are also comparable to the ocean biomes defined ~~used~~ in previous biological pump studies (e.g., Weber et al., 2016; Pasquier and Holzer, 2016).

2.3 ~~Sensitivity Analysis~~Experiments

We ~~first~~ perform a set of ~~reference experiments where the Martin curve exponents are varied between 0.4 and 1.6~~ experiments to explore the sensitivity of atmospheric CO_2 to regional variability in b with the aim to quantitatively rank the sensitivity of atmospheric CO_2 to remineralisation depth changes in each region (e.g., Pianosi et al., 2016):

1. *Control Run*: A pre-industrial control run is set up with export production diagnosed by restoring to observed surface $[PO_4]$, a globally uniform Martin exponent of 1.0 and initialised with globally uniform tracer concentrations. Atmospheric CO_2 is restored to 278 ppm. A globally uniform Martin exponent gives the lowest volume-weighted root mean square misfit compared to annual mean World Ocean Atlas 2013 $[PO_4]$ observations (Garcia et al., 2014), as found in other

studies using the same MITgcm transport matrices (Kriest et al., 2012). The control run is spun-up from uniform initial conditions for 5000 years.

2. *Global Sensitivity*: The Martin curve is varied globally, i.e., all regions are assigned the same ~~Martin curve exponent. The range is~~ exponent, between 0.4 and 1.6 in 0.1 increments, based on the range of spatial variability observed in the modern ocean (Henson et al., 2012; Marsay et al., 2015; Guidi et al., 2015). Each experiment is run for ~~10~~3,000 years ~~from initial uniform conditions~~ continuing from the control run using the nutrient-restoring scheme to predict export production (eqn. A3) ~~. We define the control run as the experiment with the lowest root mean square misfit compared to annual mean World Ocean Atlas 2013 PO_4observations (Garcia et al., 2014). We find the lowest misfit when b=1.0 globally, as found in other studies using the same MITgcm transport matrices (Kriest et al., 2012). A second set of reference experiments are then run with a constant-export scheme using the export production from the control run.~~

   ~~We perform a global sensitivity analysis with the aim to quantitatively rank the sensitivity of~~ and freely evolving atmospheric CO_2~~to remineralisation depth changes in each region (e.g., Pianosi et al., 2016).~~ .

3. *Regional Sensitivity*: Latin hypercube sampling, a stratified-random procedure that provides an efficient way of sampling high dimensional parameter space (McKay et al., 1979), is used to vary the Martin curves in every region simultaneously~~for the global sensitivity analysis.~~. Values of b are sampled from a uniform distribution ranging from 0.4 to 1.6 using the 'lhsdesign' function in MATLAB with 'maximin' sampling (an additional constraint that helps reduce clustering of samples, by maximising the minimum distance between points, in order to give a well-spread distribution of points across the parameter space). The range of b used centres around b=1.0 as used for the control run. We generate a Latin hypercube ensemble with 200 experiments, balancing the need for higher sampling resolution of the parameter space and total computational time. ~~We run two sets of the Latin hypercube experiments: one with nutrient-restoring export production and the other with constant export production where export production is taken from the control run. All experiments are run~~ Each experiment is run for 3000 years ~~following~~ continued on from the control run ~~which is sufficient for the mean deep ocean~~ with a phosphorus cycle only. Changes in atmospheric CO_2 are inferred from changes in preformed PO_4~~to equilibrate to a global change in the Martin Curve (Kwon et al., 2009). Annual mean fields of $PO_4$are~~ .

Both the global and regional sensitivity experiments are repeated with constant-export production that is diagnosed from the control run. All output is diagnosed from the last full simulation year.

2.4 Sensitivity Analysis

We use multiple linear regression analysis to derive the sensitivity of atmospheric CO_2 to changes in b in each region (k) where the fitted coefficients (β_k) give a quantitative measure of the sensitivity (e.g., Pianosi et al., 2016):

$$\mathrm{CO_2} = \beta_0 + \sum_k \beta_k b_k \tag{2}$$

3 Results

3.1 Sensitivity of CO_2 to regional variability in remineralization depths

To quantify the sensitivity of CO_2 to regional changes in b we fit linear regression models (eqn 2) to the results of the Latin hypercube ensembles. The resulting regression models explain a large proportion of the variability between CO_2 and b (R^2 = 0.88 and 0.90 for the constant-export and restoring-uptake ensembles respectively). Residuals of the regression models showed no significant bias versus the regression output (~~not shown~~Fig. S2) suggesting that a linear model was appropriate. Although the relationship between CO_2 and a globally-uniform remineralisation depth is non-linear (e.g., Fig. 6), the relationship is near linear around the observed global mean in the centre of the range of b tested (see also, Kwon et al., 2009). Overall, the absence of a strongly non-linear relationship suggests the use of a linear regression model is appropriate (Pianosi et al., 2016).

When b is varied as a globally uniform parameter from 0.4 to 1.6, atmospheric CO_2 varies from ~~219 to 303~~ 197 to 347 ppm (range of ~~84~~ 150 ppm) for the constant-export scheme and from ~~263 to 284~~ 257 to 288 ppm (range of ~~21~~ 31 ppm) for the nutrient-restoring scheme, consistent with previous model experiments (Kwon et al., 2009). Figure 3 shows how the sensitivity of CO_2 to changes in b varies as a function of region. CO_2 is most sensitive to changes in b occuring in the Subantarctic regions, with CO_2 being most sensitive to changes in the Indian sector of the Subantarctic (Fig. 3, Table 1). The Southern Ocean and sub-tropical gyres, with the exception of the gyre in the North Pacific, are consistently the regions where b has the smallest impact on CO_2. Other regions, including the equatorial Indian ocean, Equatorial Pacific and North Pacific have an intermediate sensitivity. As a region, the Subantarctic is responsible for ∼30% of the CO_2 sensitivity, comparable to the Pacific basin-scale sensitivity (Table 1).

As with the globally uniform changes in b, the magnitudes of regional sensitivities are smaller when run with nutrient-restoring uptake as opposed to a constant-export scheme because export production is able to convert any ~~changes~~ increase in surface nutrient and carbon fluxes back into organic matter, limiting any change in ~~preformed nutrients~~CO_2 fluxes. However, the relative sensitivity ranked across regions remains similar, as shown by expressing ~~b_k~~ β_k as a percentage of $\sum_k \beta_k$ (Table 1). Therefore, the regional patterns in Figure 3 are not sensitive to assumptions about the response of nutrient uptake to the redistribution of nutrients. This suggests whilst the absolute magnitude of CO_2 sensitivity to changes in b is related to global export production ~~that is is~~ it is not driven by local changes in export production specific to any region(s).

Kwon et al. (2009) demonstrated that the sensitivity of CO_2 to basin-scale changes in b correlated with the magnitude of export production in each basin. Similarly, we find a general ~~postitive relationship~~ positive correlation between sensitivity and regional export production ~~,~~ (r=0.79, $p<0.01$ for constant export, r=0.47, p=0.07 for restoring uptake), as measured by the mean annual average export production across the 200 ensemble runs (Fig 4). The correlation is much weaker with nutrient-restoring uptake compared to the constant-export production. Intuitively, regions with lower export production, i.e., that contribute less to the inventory of regenerated PO_4, have a smaller impact on the balance between preformed and regenerated nutrients and therefore on atmospheric CO_2. Whilst CO_2 is generally more sensitive to remineralisation depths in regions with higher export production, sensitivity varies across regions with similar export ~~productivity~~production. For example, the sensitivity for the temperate North Pacific (NTemp-PAC; Fig. 4a) ($\Delta CO_2/\Delta b$ = ~~15.0~~13.72, export production = 1.4±0.11 Tmol P $year^{-1}$) is approximately double that of the sub-polar region of the Southern Pacific (STemp-PAC; Fig. 4a) ($\Delta\mathrm{CO}_2/\Delta \mathrm{b}$ = ~~6.3~~5.72, export production = 1.4±0.17 Tmol P year^{-1}). There are no apparent relationships between the variability of export ~~productivity~~ production across the ensemble in each region, as shown by the horizontal errorbars, and sensitivity (Fig. 4). This further supports the finding that the response of export production to changes in nutrient distributions are not an important factor in the sensitivity of CO_2 to regional changes in b.

The variability in sensitivity not explained by the magnitude of POC export is likely a function of how changing remineralisation depths interact with ocean circulation~~to redistribute nutrients~~. To quantify this effect we calculate ~~$\overline{\mathrm{PO}_4^{\mathrm{pre}}}$~~the mean preformed PO_4 in the ocean interior derived from each region individually ($\overline{[\mathrm{P}_{\mathrm{pre}}^{region}]}$)(see Appendix A0.2) and repeat the sensitivity regression analysis:

$$\overline{[\mathrm{P}_{\mathrm{pre}}^{region}]} = \beta_0{}^r + \sum_k \beta_k{}^{region} b_k \tag{3}$$

The new regression analysis (eqn. 3) now predicts the contribution of changing b in all regions to the change in ~~$\overline{\mathrm{PO}_4^{\mathrm{pre}}}$ in~~ $\overline{[\mathrm{P}_{\mathrm{pre}}^{region}]}$ derived from a single region rather than globally (Fig. 5). ~~$\mathrm{PO}_4^{\mathrm{pre}}$ is normalised prior to the regression to make the coefficients comparable between regions which otherwise vary~~ The regression analysis is repeated for each region but the mean concentration of preformed PO_4 derived from each region varies by up to ~~three~~ four orders of magnitude ~~. As such,~~ between different regions. In order to compare regression coefficients from different regions we first normalise the concentrations ($\hat{\overline{[\mathrm{P}_{\mathrm{pre}}^{region}]}}$) to the range of variability across the 200 experiments:

$$\hat{\overline{[\mathrm{P}_{\mathrm{pre}}^{region}]}} = \frac{\overline{[\mathrm{P}_{\mathrm{pre}}^{region}]} - \min(\overline{[\mathrm{P}_{\mathrm{pre}}^{region}]})}{\max(\overline{[\mathrm{P}_{\mathrm{pre}}^{region}]}) - \min(\overline{[\mathrm{P}_{\mathrm{pre}}^{region}]})} \tag{4}$$

Figure 5 shows the relative sensitivity of ~~$\overline{\mathrm{PO}_4^{\mathrm{pre}}}$~~$\overline{[\mathrm{P}_{\mathrm{pre}}^{region}]}$ to changes in b. R^2 ranges from 0.82 to 0.97 suggesting overall the linear regression models are appropriate. The regression coefficients specific to a single region are collected from across the 15 regression results in each ~~panel~~ column of Figure 5~~to show the relative sensitivity of $\overline{\mathrm{PO}_4^{\mathrm{pre}}}$ exported across all regions in response to changes in~~. By definition, each row of Figure 5 shows the effect of changing b ~~local to the region corresponding with panel. For example, the Southern Ocean panel shows how a change in b~~ in the ~~Southern Ocean affects $\mathrm{PO}_4^{\mathrm{pre}}$ in~~ corresponding region on $\overline{[\mathrm{P}_{\mathrm{pre}}^{region}]}$ from all other regions. ~~The sensitivity locally is coloured in black and positive sensitivities indicate an increase in $\overline{\mathrm{PO}_4^{\mathrm{pre}}}$ as b increases in value, i.e., shallower remineralisation. Figure 5 displays the results for the constant-export experiments whereas the equivalent results for the restoring-uptake experiments are shown in Figure S3.~~

The sensitivity analysis for each region on an individual basis shows that changes in b in the Subantarctic regions have large impacts on ~~$\mathrm{PO}_4^{\mathrm{pre}}$~~ $\overline{[\mathrm{P}_{\mathrm{pre}}^{region}]}$ across regions globally (Fig. 5). In particular, these regions have a particular effect on the ~~$\mathrm{PO}_4^{\mathrm{pre}}$~~ $\overline{[\mathrm{P}_{\mathrm{pre}}^{region}]}$ export in the Southern Ocean and in the Atlantic as a basin, comparable in magnitude to the local changes in ~~$\mathrm{PO}_4^{\mathrm{pre}}$ (compare size of black bars to other bars: Fig. 5).~~ $\overline{[\mathrm{P}_{\mathrm{pre}}^{region}]}$. Changes in b in the equatorial upwelling regions of the Pacific and Indian Oceans also have a large global effect but with a more pronounced local effect. These features are more pronounced with nutrient-restoring uptake (Fig. ~~S3~~5b). The Southern Ocean and North Atlantic regions are those with the highest ~~$\mathrm{PO}_4^{\mathrm{pre}}$ export and variability~~ $\overline{[\mathrm{P}_{\mathrm{pre}}^{region}]}$ export across the ensemble (Table 1), consistent with previous findings about the global importance of these regions for preformed PO_4 (DeVries et al., 2012; Pasquier and Holzer, 2016). This suggests the larger ~~sensitiviy~~ sensitivity of CO_2 to changes in b in the Subantarctic regions is due to the way in which the ocean circulation connects these regions to the Southern Ocean and North Atlantic. In contrast, changing b in the Southern Ocean and North Atlantic has a relatively minimal effect on ~~$\mathrm{PO}_4^{\mathrm{pre}}$~~ $\overline{[\mathrm{P}_{\mathrm{pre}}^{region}]}$ (and by inference CO_2) both locally and globally.

3.2 Regional versus Global Sensitivity

Lastly, we explore whether the spatial patterns in sensitivity (Fig. 3) are significant on a global scale. Global average values of b are calculated for each of the 200 Latin hypercube samples using an area-weighted mean and compared against experiments where b is pertubed uniformly across regions (Fig. 6). ~~We find that the relationship between CO_2 and global mean b matches closely to that with the globally uniform b but with an offset of ∼20 ppm and ∼10 ppm for the constant and restoring export schemes respeceitively (Fig. 6a). We suggest this offset is likely caused by a non-linear relationship between b and the~~ The amount of organic matter reaching the deep ocean ~~(as measured by the e-folding depth: depth at which ∼63% of exported POC has been remineralised)~~ is a non-linear function of b, following from the fact that the Martin curve represents the scenario of a fixed remineralisation rate and an increasing sinking rate (Kriest and Oschlies, 2008; Cael and Bisson, 2018) (see Supplementary Material). ~~A change in b from 1.4 to 1.3 results in a decrease in e-folding depth of 14 m whereas a change in b from 0.4 to 0.3 results in a change of 1902 m.~~ Therefore, larger values of b, i.e., shallower remineralisation, have disproportionally more weight when ~~averaging~~ calculating a global arithmetic mean of spatially variable b values. To ~~demonstrate~~ account for this, we find the equivalent e-folding depths for each Latin hypercube sample, which form a skewed distribution due to higher occurrence of shallower remineralisation, calculate the area-weighted geometric mean e-folding depth for each sample, and re-arrange again for b (see Supplementary Material for details). ~~The distributions in Figure 6b now fall along the line of globally uniform experiments.~~

The relationship between CO_2 and the globally averaged b values from the sensitivity experiments closely matches the relationship between CO_2 and globally uniform b for the both constant-export and restoring uptake schemes (Fig. 6~~a).~~). Note that b in each region is varied within the full parameter range but that because Latin hypercube sampling varies all parameters across their parameter range simultaneously the global mean does not reach the highest and lowest global b values. The average regionally varying b values vary within $\sim\pm15$ ppm of the globally uniform experiments with constant-export and $\sim\pm5$ ppm for the nutrient-restoring experiments, comparable to the change in CO_2 for a globally uniform change in b of ∼0.2.

4 Discussion

Sediment trap observations reveal significant spatial variability in remineralisation depths. Here we have quantified the sensitivity of atmospheric CO_2 to regional changes in remineralisation depths and show that CO_2 is most sensitive to changes in the Subantarctic regions. Much of the observed spatial variability varies across latitudes (Henson et al., 2012; Guidi et al., 2015;

Marsay et al., 2015; Weber et al., 2016). Additionally, the mechanisms potentially driving these patterns are also likely to vary on a latitudinal basis, with changes in related environmental properties in response to anthropogenic CO_2 emissions affecting the high latitudes in particular: temperature changes (Kirtman et al., 2013) affecting temperature-dependent remineralisation rates; a reduction in carbonate saturation state with ocean acidification (Orr et al., 2005) affecting ballasting and changes in plankton community composition; and cell size (Lefort et al., 2015) affecting aggregation dynamics and particle sinking velocities. Additionally, this is a consideration for changes in remineralisation depths occurring in past climates (Meyer et al., 2016). This suggests that the spatial patterns in CO_2 sensitivity could be significant when considering the impact of remineralisation depth changes.

Changes in the air-sea balance of carbon are commonly related to changes in preformed nutrients. Because of the inefficient utilisation of upwelled nutrients in the Southern Ocean this region has been identified as key to setting the efficiency of the biological pump (Ito and Follows, 2005; DeVries et al., 2012). Our results show that this is also key for the the sensitivity of CO_2 to regional variability in remineralisation depths because of upwelling in the Subantarctic regions (Fig. 5). This relationship has implications when invoking changes in the efficiency of the biological pump in past climates such as the Last Glacial Maximum (LGM). Processes that increase the utilisation of nutrients in the Southern Ocean, such as iron fertilisation, and processes that reduce the delivery of nutrients to the Southern Ocean, such as increased stratification, have been implicated in the drawdown of atmospheric CO_2 during the LGM (Sigman et al., 2010). Any changes in strafication will also impact the sensitivity of CO_2 to any additional changes in remineralisation depths, such as from changes in ballasting minerals and/or temperature dependent remineralisation (Chikamoto et al., 2012). In comparison, processes such as iron fertilisation will not impact on this sensitivity. Because the spatial patterns of CO_2 sensitivity to regional changes in remineralisation are predominantly constrained by ocean circulation pathways, this also suggests that the sensitivity may change with a reorganisation of ocean circulation as suggested for the LGM (Sigman et al., 2010).

The Martin curve is a commonly used parameterisation of the remineralisation of particulate organic matter with depth in marine biogeochemical models, and is commonly applied with a globally uniform exponent (b) (Hülse et al., 2017). However, the Martin curve used in this way has potential limitations: it is an empirical and static parameterisation that does not represent the mechanisms affecting remineralisation and sinking rates; and it does not capture spatial variability in remineralisation observed in sediment trap data (Henson et al., 2012; Marsay et al., 2015; Guidi et al., 2015). In our sensitivity analysis, we have shown that CO_2 has a similar sensitivity to the global mean change in b as compared to a globally uniform change in b with an uncertainty of ±5 - 15 ppm, equivalent to a change in b of $\sim$0.2 (Fig. 6). Kwon et al. (2009) suggest a decrease of 0.3 from the modern remineralisation depth is sufficient to explain the increase in deep ocean nutrient concentrations during the Last Glacial Maximum. For the 21st century, (Laufkötter et al., 2017) predict a decrease of POC export at 500 m by 2100 under RCP8.5 in response to temperature and oxygen-dependent remineralisation, equivalent to a decrease in b of $\sim$0.25. As such, the global mean change in potential future and past changes in remineralisation depth may be larger than the uncertainty associated with spatial variability. This has potentially useful implications for modelling the remineralisation of particulate organic matter fluxes. Models resolving the various processes that affect remineralisation rates and sinking velocities have recently been developed (Jokulsdottir and Archer, 2016; Cram et al., 2018) however, the requirements to model processes such as particle aggregation can be computationally expensive, limiting their application to 1-D models (Jokulsdottir and Archer, 2016; Cram et al., 2018) or to offline models (DeVries et al., 2014). A globally uniform change in b informed by these models could then be used to calculate the impact on atmospheric CO_2 if the change in b is greater than 0.2. However, we note that the modern global mean b is subject to uncertainty associated with under-sampled spatial variability.

Our results are dependent on the use of transport matrices derived from one ~~ocean~~ global circulation model. ~~The model is commonly~~ Whilst this model has been widely applied to study biogeochemistry ~~which means that our results should be consistent with a number of existing studies (e.g., Kriest et al., 2012). In addition~~previously, it is subject to a number of caveats. The ocean model predicts significantly larger outcrops of dense water in the Southern Ocean compared to observations (see Figure S4 Duteil et al., 2013) leading to deep-water formation occurring at latitudes around 50°S (Figure S5). The volumetric fraction of water in the ocean interior derived from the Subantarctic is also higher (26%) compared with data-constrained estimates (18%: Khatiwala et al., 2012). As such, the sensitivity estimates for the Subantarctic may be over-estimated. This is also consistent with the higher sensitivity compared to the basin-scale analysis of Kwon et al. (2009) who found that the Southern Ocean (>40°S contributed 22% of the global CO_2 sensitivity, compared with 36% in this study (>38°S, Table 1). However, our results have key similarites, including absolute and relative magnitudes of regional preformed PO_4 export, to other studies using alternative steady-state ~~circulations~~ circulation states (DeVries et al., 2012; Pasquier and Holzer, 2016). As such, our results should be broadly reproducible with other models. A disadvantage to using a steady-state circulation is that we cannot quantify impact of the CO_2-climate feedback on ocean circulation and atmospheric CO_2. Studies exploring the simultaneous effects of warming temperatures on circulation and biology in response to anthropogenic CO_2 emissions show that changes in circulation could be as important as biological changes (Cao and Zhang, 2017), (but see, Yamamoto et al., 2018). Quantifying the regional sensitivity with a dynamic ocean is therefore an important focus for future ~~research. Lastly, our modelling approach uses an empirical relationship between preformed nutrients and CO_2 that enfolds the effects of processes such as air-sea gas exchange and the export of $CaCO_3$.~~ work. Ratios of $CaCO_3$ to POC vary latitudinally, and could also therefore modify our sensitivity results. Segschneider and Bendtsen (2013) found important feedbacks involving interactions between calcifiers and silicifiers in an marine ecosystem model when exploring temperature dependent remineralisation rates in the 21st Century. Future model experiments including a representation of plankton ecosystems would therefore help explore the impact of $CaCO_3$ export on regional sensitivity patterns.

5 Conclusions

We have presented a sensitivity analysis that quantifies the sensitivity of atmospheric CO_2 to regional variability in particulate organic carbon remineralisation depths. CO_2 is most sensitive to changes in remineralisation depths occurring in the Subantarctic regions, particularly the Indian Sector. As a whole, the Subantarctic regions have a sensitivity similar to that of the Pacific basin despite the smaller area and levels of ~~productivity~~production. Sensitivity patterns are in part a function of the magnitude of export production in each region and the physical circulation pathways specific to each region. Whilst the overall magnitude of CO_2 sensitivity to regional changes is dependent on the magnitude and response of export production to changes in nutrients, the relative spatial patterns in sensitivity are predominantly constrained by ocean circulation pathways. We also find that the regional variability adds ±5 - 15 ppm uncertainty to global mean changes in remineralisation depths. The regional patterns in sensitivity could be significant if a number of processes that potentially drive changes in remineralisation depths, including temperature-dependent remineralisation rates and plankton community structure, vary predominantly in the high latitudes. However, this uncertainty is similar to the change in CO_2 for a globally uniform change in b of ∼0.2 meaning that larger changes in b could be reliably approximated by a globally uniform b as commonly used in biogeochemical models.

Code and data availability. The transport matrices are publicly available at: http://kelvin.earth.ox.ac.uk/spk/Research/TMM/TransportMatrixConfigs. The model code is freely available at: http://github.com/JamieDWilson/FML

Appendix A: Model Description

The Latin hypercube sampling approach used relies on the ability to run an ensemble of model experiments. To make this approach feasible we use the 'transport matrix method' (Khatiwala et al., 2005; Khatiwala, 2007). The model is written in Fortran 90 and achieves ∼1500 years hour^{-1} on a single core.

A1 Steady-state Ocean Circulation Model

The matrix used here is the 2.8° global configuration of the MIT model with 15 vertical levels driven by seasonally cycling fluxes of momentum, heat, and freshwater, publicly available from http://kelvin.earth.ox.ac.uk/spk/Research/TMM/TransportMatrixConfig Seasonally varying ocean circulation is calculated at each timestep by linearly interpolating between monthly mean matrices. An advantage of using transport matrices is that the timestep can be made longer to reduce computational expense (Khatiwala, 2007). Here we extend the circulation timestep to 3.8 days.

A2 Biogeochemical Model

The biogeochemical model represents the cycle of phosphorus and carbon in the ocean with ~~two~~ four dissolved tracers, PO_4~~and~~ , dissolved organic phosphorus (DOP)~~..~~ , dissolved inorganic carbon (DIC) and total alkalinity. The biogeochemical model has the same timestep as the ocean circulation model (3.8 days).

A2.1 Phosphorus Cycle

PO_4 and DOP are governed by the following equations:

$$\frac{\mathrm{d}PO_4}{\mathrm{d}t} = \mathbf{A}PO_4 - J_{\mathrm{up}} + J_{\mathrm{POP}} + J_{\mathrm{DOP}} \tag{A1}$$

$$\frac{\mathrm{dDOP}}{\mathrm{d}t} = \mathbf{A}\mathrm{DOP} + \upsilon \cdot J_{\mathrm{up}} - J_{\mathrm{DOP}} \tag{A2}$$

where $\mathbf{A}$ denotes the transport matrix calculation of ocean transport and J denotes biogeochemical source/sink terms.

The uptake of PO_4 during production of organic matter occurs in the euphotic zone, here defined as the base of the upper two grid-boxes (120 m). Following Kwon et al. (2009) we calculate the production of organic matter using either a nutrient-restoring scheme or a constant-export scheme. The nutrient-restoring scheme restores surface concentrations of PO_4 to observed $[PO_4]$ with a restoring timescale (τ = 30 days Najjar et al., 2007) and is scaled by the fraction of seaice present (F_{seaice}, as monthly average fields from the original global circulation model):

$$J_{\mathrm{up}} = \frac{1}{\tau}\max\Big(\big(\mathrm{PO}_4 - \mathrm{PO}_{4,obs}\big), 0\Big)\left(1 - F_{seaice}\right) \tag{A3}$$

Organic matter production in the constant-export scheme is fixed to that of the experiment defined as the control run unless surface $[PO_4]$ is depleted below zero in which case J_{up} is set to zero at that timestep. The control run is defined as having the run with the lowest root mean square misfit compared to annual mean World Ocean Atlas $[PO_4]$ observations.

A fixed fraction (υ=0.66) of the organic matter production integrated across the upper two grid-boxes is routed directly to dissolved organic phosphorus (DOP) and remineralised back to PO_4 in a first-order reaction with decay rate κ throughout the water column:

$$J_{\mathrm{DOP}} = \kappa \mathrm{DOP} \tag{A4}$$

The remaining fraction of organic matter production ((~~1 — *kappa*~~$1-\upsilon$=0.34) is integrated across the upper two grid-boxes and exported as particulate organic phosphorus (POP) at the base of the ~~euphotic zone~~ of the second grid-box in the vertical (120 m). The remineralisation of POP is parameterised with the Martin Curve (Equation 1). POP that has reached the sediment is remineralised fully in the lowermost grid-box of the water column, maintaining a closed system with respect to $[PO_4]$. As such, there is no sediment component in this model.

Appendix B: ~~Preformed PO_4 and atmospheric CO_2~~

A0.1 Carbon Cycle

The uptake of nutrients and remineralisation of particulate and dissolved organic phosphorus are related to dissolved inorganic carbon and alkalinity via Redfield ratios of 1:16:116 (P:N:C). Carbonate chemistry parameters are computed from dissolved inorganic carbon and alkalinity using the method described by Follows et al. (2006). The method provides a simplified but accurate solution with computational efficiency. The air-sea gas exchange of CO_2 is calculated as per Orr et al. (2017).

A0.2 Preformed PO_4 and atmospheric CO_2

Changes in atmospheric CO_2 due to changes in the biological pump can be directly related to the inventory or average concentration of preformed PO_4 (~~PO_4^{pre}~~P_{pre}) if total nutrient concentrations are conserved (Ito and Follows, 2005; Marinov et al., 2008). This provides a way of relating changes in our model of the phosphorous cycle to changes in atmospheric CO_2 without simulating a relatively computationally expensive carbon cycle. The distribution of annual mean [~~PO_4^{pre}~~P_{pre}] for each run is calculated by splitting the transport matrices into "interior" matrices ($\mathbf{A^I}$) and "exterior" matrices ($\mathbf{B}$) for both the explicit and implicit matrices (subscripts e and i respectively) (see Khatiwala, 2007). The annual mean surface [PO_4] from the end of a simulation is set as a boundary condition and solving for the interior distribution of ~~PO_4^{pre}~~P_{pre}:

$$\mathbf{P}_{\mathrm{pre}} = (\mathbf{A_i^I A_e^I} - \mathbf{I})\underline{\mathbf{PO_4^{pre}} =}^{-1}((\mathbf{A_i^I B_e} + \mathbf{B_i})\mathbf{PO_4}) \tag{A1}$$

The global mean concentration of of ~~PO_4^{pre} ($\overline{[PO_4^{pre}]}$~~ P_{pre} ($\overline{[P_{pre}]}$) is related to CO_2 using a empirical quadratic function (eqn. A2) ~~. The functon~~ fitted to a series of experiments where the Martin curve is varied globally (see below). The function is derived from a ~~compilation of published PO_4^{pre} sensitivity experiments performed from three different models (Ito and Follows, 2005; Marinov et al. a~~ non-linear least squares regression (Fig. A1). ~~Although the inventories of PO_4^{pre} are model dependent (Duteil et al., 2012), the changes in $\overline{[PO_4^{pre}]}$ and CO_2 relative to those of the control run show consistent trends across the different models.~~ The resulting regression fit (details in Figure caption) is used to estimate changes in CO_2:

$$CO_2 = (\beta_1 \underline{\Delta PO_4^{pre\,2}}\,\overline{[P_{pre}]}^2 + \beta_2 \underline{\Delta PO_4^{pre}}\,\overline{[P_{pre}]} + \beta_3)\underline{+CO_2^{ctrl}} \tag{A2}$$

Author contributions. JDW designed the experiments, developed the model code and ran the model. JDW prepared the manuscript with input from all co-authors.

Competing interests. The authors declare that they have no conflict of interest.

Acknowledgements. This work is based on work originally conducted as part of a PhD project (JDW) associated with the UK Ocean Acidification Research Programme (UKOARP), grant NE/H017240/1 to AR and SB. JDW and AR acknowledge support via the EU grant ERC-2013-Cog-617313. We would like to thank Andrew Yool for his comments on an earlier version of the manuscript. We also thank Samar Khatiwala for making transport matrices freely available.

References

Boyd, P. W.: Toward quantifying the response of the oceans' biological pump to climate change, Frontiers in Marine Science, 2, 77, https://doi.org/10.3389/fmars.2015.00077, http://journal.frontiersin.org/article/10.3389/fmars.2015.00077, 2015.

Cael, B. B. and Bisson, K.: Particle Flux Parameterizations: Quantitative and Mechanistic Similarities and Differences, Frontiers in Marine Science, 5, 395, https://doi.org/10.3389/fmars.2018.00395, https://www.frontiersin.org/article/10.3389/fmars.2018.00395, 2018.

Cao, L. and Zhang, H.: The role of biological rates in the simulated warming effect on oceanic CO_2 uptake, Journal of Geophysical Research: Biogeosciences, 122, 1098–1106, https://doi.org/10.1002/2016JG003756, http://dx.doi.org/10.1002/2016JG003756, 2017.

Chikamoto, M. O., Abe-Ouchi, A., Oka, A., and Smith, S. L.: Temperature-induced marine export production during glacial period, Geophysical Research Letters, 39, L21 601, https://doi.org/10.1029/2012GL053828, http://dx.doi.org/10.1029/2012GL053828, 2012.

Cram, J. A., Weber, T., Leung, S. W., McDonnell, A. M. P., Liang, J.-H., and Deutsch, C.: The Role of Particle Size, Ballast, Temperature, and Oxygen in the Sinking Flux to the Deep Sea, Global Biogeochemical Cycles, 32, 858–876, https://doi.org/10.1029/2017GB005710, https://agupubs.onlinelibrary.wiley.com/doi/abs/10.1029/2017GB005710, 2018.

DeVries, T., Primeau, F., and Deutsch, C.: The sequestration efficiency of the biological pump, Geophysical Research Letters, 39, https://doi.org/10.1029/2012GL051963, http://dx.doi.org/10.1029/2012GL051963, l13601, 2012.

DeVries, T., Liang, J.-H., and Deutsch, C.: A mechanistic particle flux model applied to the oceanic phosphorus cycle, Biogeosciences, 11, 5381–5398, https://doi.org/10.5194/bg-11-5381-2014, http://www.biogeosciences.net/11/5381/2014/, 2014.

Duteil, O., Koeve, W., Oschlies, A., Aumont, O., Bianchi, D., Bopp, L., Galbraith, E., Matear, R., Moore, J. K., Sarmiento, J. L., and Segschneider, J.: Preformed and regenerated phosphate in ocean general circulation models: can right total concentrations be wrong?, Biogeosciences, 9, 1797–1807, https://doi.org/10.5194/bg-9-1797-2012, http://www.biogeosciences.net/9/1797/2012/, 2012.

Duteil, O., Koeve, W., Oschlies, A., Bianchi, D., Galbraith, E., Kriest, I., and Matear, R.: A novel estimate of ocean oxygen utilisation points to a reduced rate of respiration in the ocean interior, Biogeosciences, 10, 7723–7738, https://doi.org/10.5194/bg-10-7723-2013, http://www.biogeosciences.net/10/7723/2013/, 2013.

Fay, A. R. and McKinley, G. A.: Global open-ocean biomes: mean and temporal variability, Earth System Science Data, 6, 273–284, https://doi.org/10.5194/essd-6-273-2014, http://www.earth-syst-sci-data.net/6/273/2014/, 2014.

Follows, M. J., Ito, T., and Dutkiewicz, S.: On the solution of the carbonate chemistry system in ocean biogeochemistry models, Ocean Modelling, 12, 290 – 301, https://doi.org/https://doi.org/10.1016/j.ocemod.2005.05.004, http://www.sciencedirect.com/science/article/pii/S1463500305000533, 2006.

Garcia, H. E., Locarnini, R. A., Boyer, T. P., Antonov, J. I., Baranova, O. K., Zweng, M. M., Reagan, J. R., and Johnson, D. R.: World Ocean Atlas 2013, Volume 4: Dissolved Inorganic Nutrients (phosphate, nitrate, silicate)., in: NOAA Atlas NESDIS, edited by Levitus, S., U.S. Government Printing Office, Washington, D.C., 2014.

Gloor, M., Gruber, N., Hughes, T. M. C., and Sarmiento, J. L.: Estimating net air-sea fluxes from ocean bulk data: Methodology and application to the heat cycle, Global Biogeochemical Cycles, 15, 767–782, https://doi.org/10.1029/2000GB001301, http://dx.doi.org/10.1029/2000GB001301, 2001.

Guidi, L., Legendre, L., Reygondeau, G., Uitz, J., Stemmann, L., and Henson, S. A.: A new look at ocean carbon remineralization for estimating deepwater sequestration, Global Biogeochemical Cycles, pp. n/a–n/a, https://doi.org/10.1002/2014GB005063, http://dx.doi.org/10.1002/2014GB005063, 2014GB005063, 2015.

Henson, S., Sanders, R., and Madsen, E.: Global patterns in efficiency of particulate organic carbon export and transfer to the deep ocean, Global Biogeochemical Cycles, 26, GB1028, https://doi.org/10.1029/2011GB004099, 2012.

Henson, S. A., Sarmiento, J. L., Dunne, J. P., Bopp, L., Lima, I., Doney, S. C., John, J., and Beaulieu, C.: Detection of anthropogenic climate change in satellite records of ocean chlorophyll and productivity, Biogeosciences, 7, 621–640, https://doi.org/10.5194/bg-7-621-2010, http://www.biogeosciences.net/7/621/2010/, 2010.

Henson, S. A., Sanders, R., Madsen, E., Morris, P. J., Le Moigne, F., and Quartly, G. D.: A reduced estimate of the strength of the ocean's biological carbon pump, Geophysical Research Letters, 38, L04 606, https://doi.org/10.1029/2011GL046735, http://dx.doi.org/10.1029/2011GL046735, 2011.

Hülse, D., Arndt, S., Wilson, J. D., Munhoven, G., and Ridgwell, A.: Understanding the causes and consequences of past marine carbon cycling variability through models, Earth-Science Reviews, 171, 349 – 382, https://doi.org/https://doi.org/10.1016/j.earscirev.2017.06.004, http://www.sciencedirect.com/science/article/pii/S0012825216303191, 2017.

Ito, T. and Follows, M. J.: Preformed phosphate, soft-tissue pump and atmospheric CO_2, Journal of Marine Research, 64, 813 – 839, 2005.

John, E., Wilson, J., Pearson, P., and Ridgwell, A.: Temperature-dependent remineralization and carbon cycling in the warm Eocene oceans, Palaeogeography, Palaeoclimatology, Palaeoecology, 413, 158 – 166, https://doi.org/http://dx.doi.org/10.1016/j.palaeo.2014.05.019, http://www.sciencedirect.com/science/article/pii/S0031018214002685, 2014.

Jokulsdottir, T. and Archer, D.: A stochastic, Lagrangian model of sinking biogenic aggregates in the ocean (SLAMS 1.0): model formulation, validation and sensitivity, Geoscientific Model Development, 9, 1455–1476, https://doi.org/10.5194/gmd-9-1455-2016, http://www.geosci-model-dev.net/9/1455/2016/, 2016.

Khatiwala, S.: A computational framework for simulation of biogeochemical tracers in the ocean, Global Biogeochemical Cycles, 21, GB3001, https://doi.org/10.1029/2007GB002923, http://dx.doi.org/10.1029/2007GB002923, 2007.

Khatiwala, S., Visbeck, M., and Cane, M. A.: Accelerated simulation of passive tracers in ocean circulation models, Ocean Modelling, 9, 51 – 69, https://doi.org/http://dx.doi.org/10.1016/j.ocemod.2004.04.002, http://www.sciencedirect.com/science/article/pii/S1463500304000307, 2005.

Khatiwala, S., Primeau, F., and Holze, M.: Ventilation of the deep ocean constrained with tracer observations and implications for radiocarbon estimates of ideal mean age, Earth and Planetary Science Letters, 325-326, 116 – 125, https://doi.org/doi:10.1016/j.epsl.2012.01.038, http://www.sciencedirect.com/science/article/pii/S0012821X12000672, 2012.

Kirtman, B., Power, S., Adedoyin, J., Boer, G., Bojariu, R., Camilloni, I., Doblas-Reyes, F., Fiore, A., Kimoto, M., Meehl, G., Prather, M., Sarr, A., Schar, C., Sutton, R., van Oldenborgh, G., Vecchi, G., and Wang, H.: Near-term Climate Change: Projections and Predictability, in: Climate Change 2013: The Physical Science Basis. Contribution of Working Group I to the Fifth Assessment Report of the Intergovernmental Panel on Climate Change, edited by Stocker, T., Qin, D., Plattner, G.-K., Tignor, M., Allen, S., Boschung, J., Nauels, A., Xia, Y., Bex, V., and Midgley, P., Cambridge University Press, http://www.ipcc.ch/report/ar5/wg1/, 2013.

Kriest, I. and Oschlies, A.: On the treatment of particulate organic matter sinking in large-scale models of marine biogeochemical cycles, Biogeosciences, 5, 55–72, https://doi.org/10.5194/bg-5-55-2008, http://www.biogeosciences.net/5/55/2008/, 2008.

Kriest, I. and Oschlies, A.: MOPS-1.0: towards a model for the regulation of the global oceanic nitrogen budget by marine biogeochemical processes, Geoscientific Model Development, 8, 2929–2957, https://doi.org/10.5194/gmd-8-2929-2015, http://www.geosci-model-dev.net/8/2929/2015/, 2015.

Kriest, I., Oschlies, A., and Khatiwala, S.: Sensitivity analysis of simple global marine biogeochemical models, Global Biogeochemical Cycles, 26, GB2029, https://doi.org/10.1029/2011GB004072, http://dx.doi.org/10.1029/2011GB004072, 2012.

Kwon, E. Y., Primeau, F., and Sarmiento, J. L.: The impact of remineralization depth on the air-sea carbon balance, Nature Geoscience, 2, 630–635, http://dx.doi.org/10.1038/ngeo612, 2009.

Lam, P. J., Doney, S. C., and Bishop, J. K. B.: The dynamic ocean biological pump: Insights from a global compilation of particulate organic carbon, $CaCO_3$, and opal concentration profiles from the mesopelagic, Global Biogeochemical Cycles, 25, GB3009, https://doi.org/10.1029/2010GB003868, 2011.

Laufkötter, C., John, J. G., Stock, C. A., and Dunne, J. P.: Temperature and oxygen dependence of the remineralization of organic matter, Global Biogeochemical Cycles, 31, 1038–1050, https://doi.org/10.1002/2017GB005643, http://dx.doi.org/10.1002/2017GB005643, 2017GB005643, 2017.

Lefort, S., Aumont, O., Bopp, L., Arsouze, T., Gehlen, M., and Maury, O.: Spatial and body-size dependent response of marine pelagic communities to projected global climate change, Global Change Biology, 21, 154–164, https://doi.org/10.1111/gcb.12679, http://dx.doi.org/10.1111/gcb.12679, 2015.

Longhurst, A.: Ecological Geography of the Sea, Academic Press, San Diego, 1998.

Marinov, I., Gnanadesikan, A., Sarmiento, J. L., Toggweiler, J. R., Follows, M., and Mignone, B. K.: Impact of oceanic circulation on biological carbon storage in the ocean and atmospheric pCO_2, Global Biogeochemical Cycles, 22, GB3007, https://doi.org/10.1029/2007GB002958, http://dx.doi.org/10.1029/2007GB002958, 2008.

Marsay, C., Sanders, R., Henson, S., Pabortsava, K., Achterberg, E., and Lampitt, R.: Attenuation of sinking particulate organic carbon flux through the mesopelagic ocean, Proceedings of the National Academy of Sciences, 112, 1089–1094, https://doi.org/10.1073/pnas.1415311112, http://www.pnas.org/content/112/4/1089.abstract, 2015.

Martin, J., Knauer, G., Karl, D., and Broenkow, W.: VERTEX: carbon cycling in the northeast Pacific, Deep Sea Research, 43, 267 – 285, 1987.

McKay, M. D., Beckman, R. J., and Conover, W. J.: A Comparison of Three Methods for Selecting Values of Input Variables in the Analysis of Output From a Computer Code, Technometrics, 21, 239 – 245, 1979.

Meyer, K. M., Ridgwell, A., and Payne, J. L.: The influence of the biological pump on ocean chemistry: implications for long-term trends in marine redox chemistry, the global carbon cycle, and marine animal ecosystems, Geobiology, 14, 207–219, https://doi.org/10.1111/gbi.12176, http://dx.doi.org/10.1111/gbi.12176, 2016.

Mikaloff Fletcher, S. E., Gruber, N., Jacobson, A. R., Doney, S. C., Dutkiewicz, S., Gerber, M., Follows, M., Joos, F., Lindsay, K., Menemenlis, D., Mouchet, A., Müller, S. A., and Sarmiento, J. L.: Inverse estimates of anthropogenic CO_2 uptake, transport, and storage by the ocean, Global Biogeochemical Cycles, 20, GB2002, https://doi.org/10.1029/2005GB002530, http://dx.doi.org/10.1029/2005GB002530, 2006.

Najjar, R. G., Jin, X., Louanchi, F., Aumont, O., Caldeira, K., Doney, S. C., Dutay, J.-C., Follows, M., Gruber, N., Joos, F., Lindsay, K., Maier-Reimer, E., Matear, R. J., Matsumoto, K., Monfray, P., Mouchet, A., Orr, J. C., Plattner, G.-K., Sarmiento, J. L., Schlitzer, R., Slater, R. D., Weirig, M.-F., Yamanaka, Y., and Yool, A.: Impact of circulation on export production, dissolved organic matter, and dissolved oxygen in the ocean: Results from Phase II of the Ocean Carbon-cycle Model Intercomparison Project (OCMIP-2), Global Biogeochemical Cycles, 21, GB3007, https://doi.org/10.1029/2006GB002857, http://dx.doi.org/10.1029/2006GB002857, 2007.

Orr, J. C., Fabry, V. J., Aumont, O., Bopp, L., Doney, S. C., Feely, R. A., Gnanadesikan, A., Gruber, N., Ishida, A., Joos, F., Key, R. M., Lindsay, K., Maier-Reimer, E., Matear, R., Monfray, P., Mouchet, A., Najjar, R. G., Plattner, G.-K., Rodgers, K. B., Sabine, C. L., Sarmiento, J. L., Schlitzer, R., Slater, R. D., Totterdell, I. J., Weirig, M.-F., Yamanaka, Y., and Yool, A.: Anthropogenic ocean acidification over the twenty-first century and its impact on calcifying organisms, Nature, 437, 681–686, https://doi.org/10.1038/nature04095, 2005.

Orr, J. C., Najjar, R. G., Aumont, O., Bopp, L., Bullister, J. L., Danabasoglu, G., Doney, S. C., Dunne, J. P., Dutay, J.-C., Graven, H., Griffies, S. M., John, J. G., Joos, F., Levin, I., Lindsay, K., Matear, R. J., McKinley, G. A., Mouchet, A., Oschlies, A., Romanou, A., Schlitzer, R., Tagliabue, A., Tanhua, T., and Yool, A.: Biogeochemical protocols and diagnostics for the CMIP6 Ocean Model Intercomparison Project (OMIP), Geoscientific Model Development, 10, 2169–2199, https://doi.org/10.5194/gmd-10-2169-2017, https://www.geosci-model-dev.net/10/2169/2017/, 2017.

Pasquier, B. and Holzer, M.: The plumbing of the global biological pump: Efficiency control through leaks, pathways, and time scales, Journal of Geophysical Research: Oceans, 121, 6367–6388, https://doi.org/10.1002/2016JC011821, https://agupubs.onlinelibrary.wiley.com/doi/abs/10.1002/2016JC011821, 2016.

Pianosi, F., Beven, K., Freer, J., Hall, J. W., Rougier, J., Stephenson, D. B., and Wagener, T.: Sensitivity analysis of environmental models: A systematic review with practical workflow, Environmental Modelling & Software, 79, 214 – 232, https://doi.org/http://dx.doi.org/10.1016/j.envsoft.2016.02.008, http://www.sciencedirect.com/science/article/pii/S1364815216300287, 2016.

Riebesell, U., Kortzinger, A., and Oschlies, A.: Sensitivities of marine carbon fluxes to ocean change, Proceedings of the National Academy of Sciences of the United States of America, 106, 20 602–20 609, https://doi.org/10.1073/pnas.0813291106, 2009.

Roth, R., Ritz, S. P., and Joos, F.: Burial-nutrient feedbacks amplify the sensitivity of atmospheric carbon dioxide to changes in organic matter remineralisation, Earth System Dynamics, 5, 321–343, https://doi.org/10.5194/esd-5-321-2014, http://www.earth-syst-dynam.net/5/321/2014/, 2014.

Sarmiento, J. L., Slater, R., Barber, R., Bopp, L., Doney, S. C., Hirst, A. C., Kleypas, J., Matear, R., Mikolajewicz, U., Monfray, P., Soldatov, V., Spall, S. A., and Stouffer, R.: Response of ocean ecosystems to climate warming, Global Biogeochemical Cycles, 18, GB3003, https://doi.org/10.1029/2003GB002134, http://dx.doi.org/10.1029/2003GB002134, 2004.

Segschneider, J. and Bendtsen, J.: Temperature-dependent remineralization in a warming ocean increases surface pCO_2 through changes in marine ecosystem composition, Global Biogeochemical Cycles, 27, 1214–1225, https://doi.org/10.1002/2013GB004684, http://dx.doi.org/10.1002/2013GB004684, 2013.

Sigman, D. M., Hain, M. P., and Haug, G. H.: The polar ocean and glacial cycles in atmospheric CO_2 concentration, Nature, 466, 47–55, http://dx.doi.org/10.1038/nature09149, 2010.

Weber, T., Cram, J., Leung, S., DeVries, T., and Deutsch, C.: Deep ocean nutrients imply large latitudinal variation in particle transfer efficiency, Proceedings of the National Academy of Sciences, 113, 8606 – 611, 2016.

Yamamoto, A., Abe-Ouchi, A., and Yamanaka, Y.: Long-term response of oceanic carbon uptake to global warming via physical and biological pumps, Biogeosciences, 15, 4163–4180, https://doi.org/10.5194/bg-15-4163-2018, https://www.biogeosciences.net/15/4163/2018/, 2018.

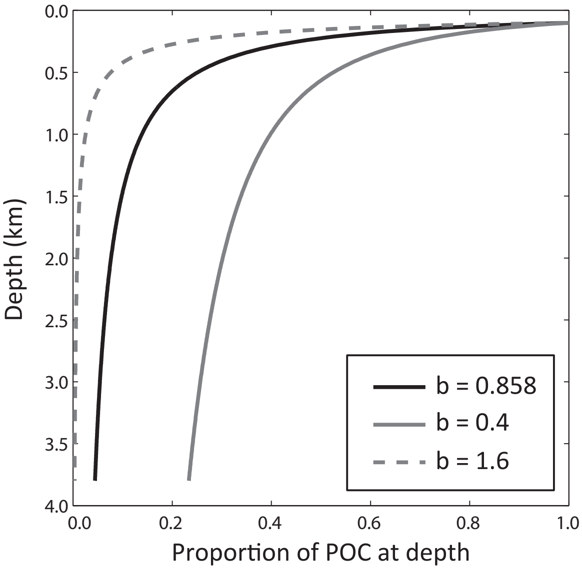

Figure 1. The normalised water column distribution of particulate fluxes defined using the Martin curve. As a comparison, Martin curves are shown with the exponent found by Martin et al. (1987) (b=0.858) and minimum and maximum exponent values used in this study based on sediment trap data compilations (b=0.4, b=1.6 Henson et al., 2012; Marsay et al., 2015; Guidi et al., 2015). All curves have export depth (z_0, eqn. 1) of 120 m.

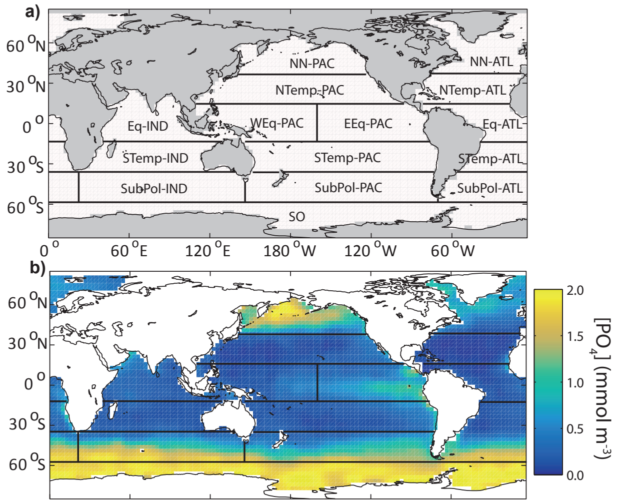

Figure 2. a) Location and names of the 15 regions defined on the model grid based on Gloor et al. (2001). Boundaries are at 58°S, 36°S, 13°S, 13°N, and 36°N. The equatorial Pacific is split at 98.75°E following Mikaloff Fletcher et al. (2006). Each region can be assigned a value of b that is independent of other regions. b) Location of regions superimposed on the annual mean surface [PO_4] from World Ocean Atlas 13 (Garcia et al., 2014) regridded to the model grid.

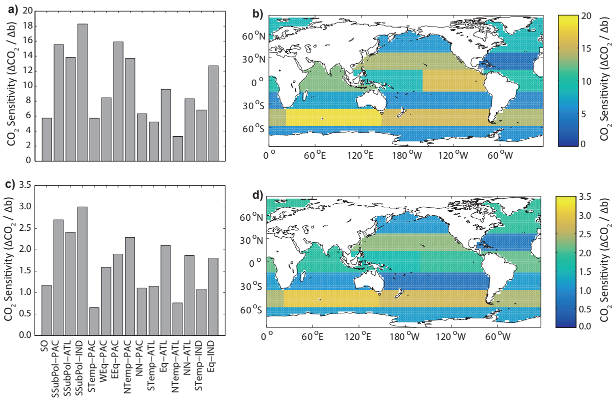

Figure 3. Regional sensitivity ($\Delta CO_2/\Delta b$) of atmospheric CO_2 (ppm) to changes in Martin ~~curve exponents (*b*: unitless)~~ curves for ~~(a)~~ the constant-export scheme ~~and~~ (panels a & b) ~~the~~ and restoring-uptake scheme (panels c & d). ~~A positive~~ The sensitivity value ~~relects an~~ reflects the increase in CO_2 (preformed PO_4) ~~with increasing~~ for an increase in b (shallower remineralisation). Atmospheric CO_2 is inferred from modelled preformed PO_4 using ~~the~~ empirical ~~relationship~~ relationships in Figure A1.

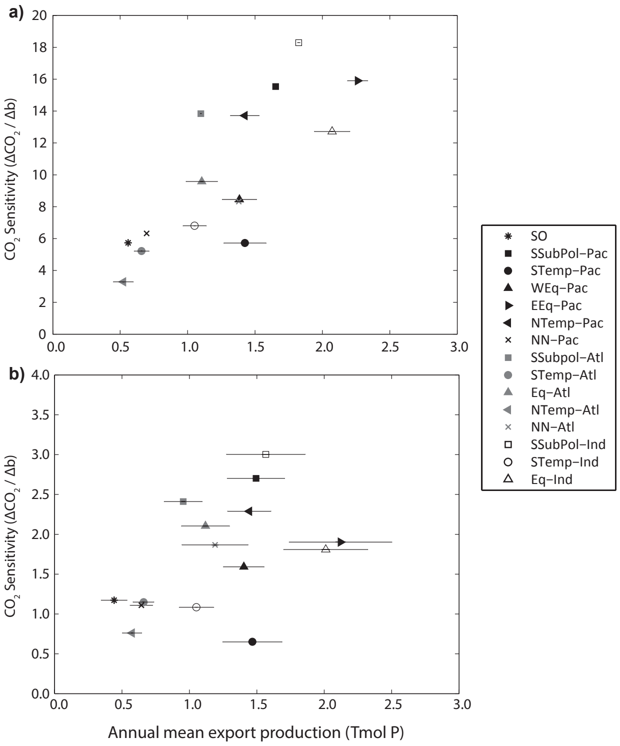

Figure 4. Relationship between regional CO$_2$ sensitivity and annual export of PO$_4$ in each region using (a) the constant-export scheme and (b) the restoring-uptake scheme. Annual export is shown as the mean of the 200 ensemble experiments with ±1 standard deviation error bars.

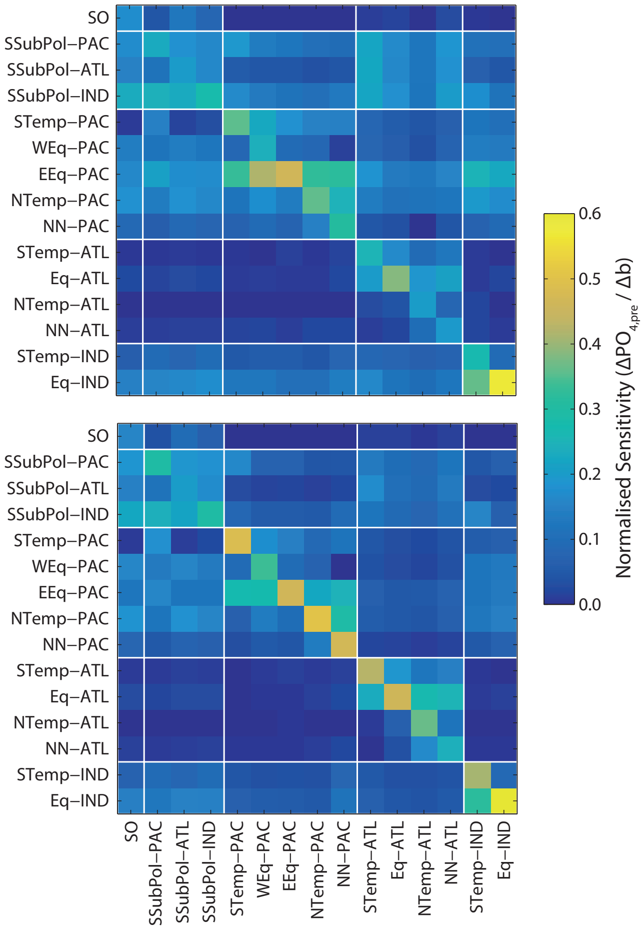

Figure 5. ~~Normalised sensitivity~~ Sensitivity of steady-state normalised mean preformed $[\mathrm{PO}_4]$ ~~in all regions to~~ exported from each region ($\overline{[\mathrm{P}_{\mathrm{pre}}^{region}]}$). $\overline{[\mathrm{P}_{\mathrm{pre}}^{region}]}$ from each region is expressed as a ~~local change in~~ function of b ~~calculated with the constant-export scheme~~using linear regression. ~~Sensitivity~~ $\overline{[\mathrm{P}_{\mathrm{pre}}^{region}]}$ is ~~calculated using equation 3 and preformed $\mathrm{PO}_4$is~~ normalised ~~before so that sensitivity can be compared on~~ to the ~~same scale~~range of values within each region in the ensemble to account for large differences in preformed $\overline{[\mathrm{P}_{\mathrm{pre}}^{region}]}$ between regions. The regression coefficients ~~specific to a single region~~ are ~~collected from across the 15 regression results in~~ arranged such that each ~~panel to show~~ row shows the ~~relative sensitivity~~ impact of ~~$\mathrm{PO}_4^{\mathrm{pre}}$ exported across all regions (grey) in response to changes in~~ changing b ~~local to the~~ in that region ~~(black) corresponding with panel~~on $\overline{[\mathrm{P}_{\mathrm{pre}}^{region}]}$ across other regions. ~~Panels are arranged by basins and by latitude.~~ The ~~equivalent plot~~ upper and lower panels show the results for the constant-export and restoring-uptake ~~scheme is found in the supplementary material~~schemes respectively.

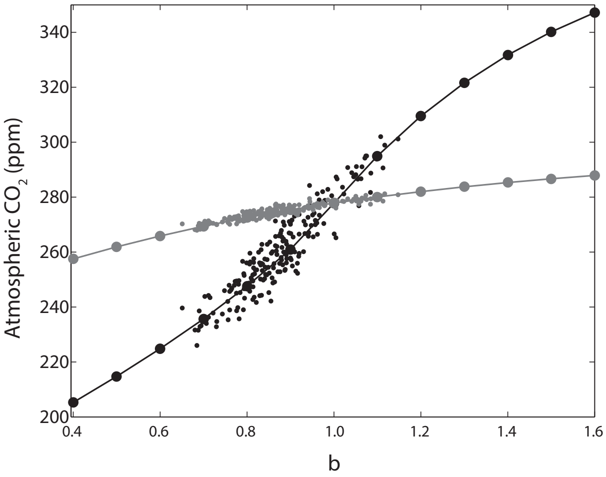

Figure 6. Comparison of CO$_2$ sensitivity when b is varied as globally uniform parameter (solid lines) and when b is varied regionally in the Latin hypercube samples and calculated as an ~~(a)~~ area-weighted ~~global mean and (b) area-weighted~~ geometric mean of e-folding depths converted back to b to correct for non-linearities in the Martin Curve. Runs using the constant-export scheme are shown in black and restoring-uptake runs are shown in grey.

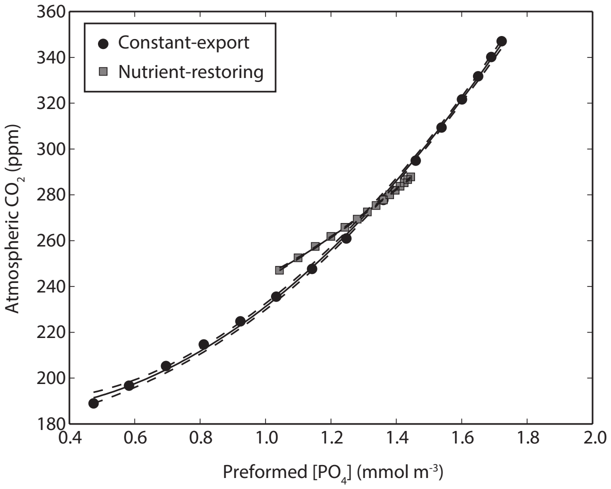

Figure A1. Relationship between ~~relative changes in~~ preformed PO_4 and atmospheric CO_2 ~~from previously published~~ in the biogeochemical model ~~experiments (see legend for details). Relative changes are calculated by subtracting~~ using nutrient-restoring and constant-export when the ~~respective values from the control run (for Marinov et al., 2008 this~~ Martin curve is ~~defined as the LL - regular gas exchange run). All models feature gas exchange~~ varied globally between 0.4 and ~~no export production of $CaCO_3$~~1.6. A quadratic function ($\Delta CO_2 = \beta_1 \Delta PO_{4,pre}{}^2 + \beta_2 \Delta PO_{4,pre} + \beta_3$) is fitted to the combined data with non-linear least squares is shown with 95 % confidence intervals. The ~~R^2 for the regression model is 0.97. The~~ coefficients for the ~~fit~~ two fits are β_1=~~54.12~~66.59, β_2=~~170.15~~ -22.48 and β_3=~~1.37~~187.09 for constant-export and β_1=42.80, β_2=-6.69 and β_3=207.95

Table 1. Key metrics and sensitivity estimates for each region and basins. Representative metrics including area (% of global area), region-integrated mean annual ~~POC~~ POP export (% of global POP export), and mean preformed [PO_4] (% of global mean) are taken from the control run~~,~~. CO_2 sensitivity estimates for both the restoring-uptake and constant-export ensembles given as $\Delta CO_2/\Delta b$) (β_k from eqn. 2) and as a % ($\beta_k/\sum_k \beta_k$)

	~~area~~	Control	Constant Export			Restoring Uptake
	Area (%)	~~POC~~ POP Export (%) ~~[a]~~	~~β ($\Delta CO_2/\Delta b$~~ $PO_{4,pre}$ (%)	~~β (~~ β_k ($\Delta CO_2/\Delta b$)	$\beta_k/\sum_k \beta_k$ (%)	~~β ($\Delta CO_2/\Delta b$~~ β_k (Δ
SO	6.70	2.81	~~6.40~~ 40.20	~~3.89~~ 5.73	~~1.83~~ 3.83	~~4.59~~ 1.17
SubPol-PAC	7.67	8.35	~~17.11~~ 5.23	15.54	10.40	~~4.20~~ 2.70
STemp-PAC	10.37	7.86	~~6.25~~ 0.29	~~3.80~~ 5.72	~~1.01~~ 3.83	0.65
Weq-PAC	7.21	7.46	~~9.42~~ 0.11	~~5.72~~ 8.45	~~2.48~~ 5.66	~~6.23~~ 1.59
Eeq-PAC	8.20	11.53	~~17.45~~ 0.24	~~10.60~~ 15.91	~~2.96~~ 10.64	1.90
Ntemp-PAC	9.69	7.66	~~15.04~~ 0.26	~~9.14~~ 13.72	~~3.56~~ 9.18	2.29
NN-PAC	4.94	3.50	~~6.99~~ 4.21	~~4.25~~ 6.32	~~1.73~~ 4.23	~~4.34~~ 1.11
SubPol-ATL	4.84	5.52	~~15.23~~ 12.22	~~9.25~~ 13.84	~~3.75~~ 9.26	2.41
Stemp-ATL	4.46	3.53	~~5.79~~ 0.14	~~3.52~~ 5.21	~~1.79~~ 3.49	1.15
Eq-ATL	5.45	6.06	~~10.58~~ 0.10	~~6.43~~ 9.58	~~3.28~~ 6.41	2.10
NTemp-ATL	5.13	3.09	~~3.44~~ 0.04	~~2.09~~ 3.29	~~1.18~~ 2.20	~~2.96~~ 0.76
NN-ATL	4.84	7.04	~~9.16~~ 23.54	8.32	5.57	~~2.91~~ 1.87
SubPol-IND	6.86	9.18	~~20.26~~ 13.04	~~12.31~~ 18.29	~~4.68~~ 12.24	3.00
STemp-IND	6.31	5.63	~~7.47~~ 0.20	~~4.54~~ 6.80	~~1.69~~ 4.55	1.08
Eq-IND	7.32	10.85	~~13.98~~ 0.20	~~8.49~~ 12.72	~~2.81~~ 8.51	1.81
>38°S[a]	26.08	25.85	70.68	53.40	35.73	9.29
Subantarctic[b]	19.38	23.04	~~n/a~~ 30.48	~~31.96~~ 47.67	~~n/a~~ 31.90	8.11
Pacific	40.41	37.96	~~n/a~~ 5.11	~~33.52~~ 50.11	~~n/a~~ 33.54	~~29.47~~ 7.54
Atlantic	19.88	19.72	~~n/a~~ 23.81	~~17.60~~ 26.40	~~n/a~~ 17.67	5.88
Indian	13.63	16.48	~~n/a~~ 0.40	~~13.03~~ 19.52	~~n/a~~ 13.06	~~11.29~~ 2.89

[a] For comparison with Southern Ocean estimate defined as >40°S in Kwon et al. (2009) [b] SubPol-PAC, SubPol-ATL and SubPol-IND